



Theses and Dissertations

---

2008-07-17

## Quantitative Uncertainty of Chemical Plume Transport in Low Wind Speeds Using Measured Field Data and Stochastic Modeling

Veronica Elaine Wannberg  
*Brigham Young University - Provo*

Follow this and additional works at: <https://scholarsarchive.byu.edu/etd>



Part of the [Civil and Environmental Engineering Commons](#)

---

### BYU ScholarsArchive Citation

Wannberg, Veronica Elaine, "Quantitative Uncertainty of Chemical Plume Transport in Low Wind Speeds Using Measured Field Data and Stochastic Modeling" (2008). *Theses and Dissertations*. 1869.  
<https://scholarsarchive.byu.edu/etd/1869>

This Thesis is brought to you for free and open access by BYU ScholarsArchive. It has been accepted for inclusion in Theses and Dissertations by an authorized administrator of BYU ScholarsArchive. For more information, please contact [scholarsarchive@byu.edu](mailto:scholarsarchive@byu.edu), [ellen\\_amatangelo@byu.edu](mailto:ellen_amatangelo@byu.edu).

QUANTITATIVE UNCERTAINTY OF CHEMICAL  
PLUME TRANSPORT IN LOW WIND SPEEDS  
USING MEASURED FIELD DATA AND  
STOCHASTIC MODELING

by

Veronica E. Wannberg

A thesis submitted to the faculty of

Brigham Young University

in partial fulfillment of the requirements for the degree of

Master of Science

Department of Civil and Environmental Engineering

Brigham Young University

August 2008



BRIGHAM YOUNG UNIVERSITY

GRADUATE COMMITTEE APPROVAL

of a thesis submitted by

Veronica E. Wannberg

This thesis has been read by each member of the following graduate committee and by majority vote has been found to be satisfactory.

\_\_\_\_\_

Date

\_\_\_\_\_

Gustavious P. Williams, Chair

\_\_\_\_\_

Date

\_\_\_\_\_

E. James Nelson, Member

\_\_\_\_\_

Date

\_\_\_\_\_

M. Brett Borup, Member



BRIGHAM YOUNG UNIVERSITY

As chair of the candidate's graduate committee, I have read the thesis of Veronica E. Wannberg in its final form and have found that (1) its format, citations, and bibliographical style are consistent and acceptable and fulfill university and department style requirements; (2) its illustrative materials including figures, tables, and charts are in place; and (3) the final manuscript is satisfactory to the graduate committee and is ready for submission to the university library.

---

Date

---

Gustavious P. Williams  
Chair, Graduate Committee

Accepted for the Department

---

E. James Nelson  
Graduate Coordinator

Accepted for the College

---

Alan R. Parkinson  
Dean, Ira A. Fulton College of Engineering  
and Technology



## ABSTRACT

# QUANTITATIVE UNCERTAINTY OF CONTAMINANT PLUME TRANSPORT IN LOW WIND SPEEDS USING MEASURED FIELD DATA AND STOCHASTIC MODELING

Veronica E. Wannberg

Department of Civil and Environmental Engineering

Master of Science

Low wind speed conditions should be studied because these conditions can present risk, particularly for areas immediately surrounding the release point, where high concentrations can occur and not dissipate. The following research attempts to clarify the processes governing both the general and low wind speed cases by determining the accuracy and uncertainty of standard prediction methods for contaminant plume transport in low wind speed plume modeling.

Multiple techniques were utilized to incorporate field measured data, previously gathered for a different purpose, to generate parameter distributions and ground-truth data that could be used in stochastic models for chemical plume prediction. These data were



taken during a multi-day experiment performed on Frenchman Flats, a flat, dry lakebed, at the Nevada Test Site (NTS) in February of 2007 and include weather data and chemical concentrations throughout the chemical release time.

I organized these data into continuous time series for each sampling location, which were represented as vectors for the statistical and mathematical analysis. I then animated these vectors with respect to time and performed a stochastic analysis which I compared to these observed vectors. Predicted vectors of chemical concentrations, based on the statistical parameter distributions generated from the observed vectors were developed and a statistical analysis was performed on the results of the stochastic process to determine how well the model predicted the plume.

It was found that stochastically modeling, with SCIPuff, of contaminant plume releases in low wind speed conditions is not accurate. This was expected because below 2 m/s, plumes no longer have a Gaussian distribution and are difficult to predict because of fluctuating winds. In fact, the model only accurately predicts the period before the plume arrives at the sensor when no plume is present.

It is possible, and even probable, that stochastic modeling of contaminant plumes will provide a means to compute the bounds of a release, when coupled with a model that is accurate for low wind speed conditions and includes all the complexities of the wind field.

An unexpected finding is the fact that the vertical dimension of wind movement cannot be ignored in low wind speed conditions. When planning future experiments, special attention should be paid to obtaining a good representation of the 3-D wind profile.



## ACKNOWLEDGMENTS

I would like to thank the following people.

Dr. Williams for his unending help, direction, and 733T programming skillz.

Pat Sawyer for designing the experiment and letting me latch on and take the analysis a little farther. Congratulations on finishing your Masters! Good luck with the PhD program.

NTE for funding my research and thesis, Gus' access, and for letting me come and visit the Test Site.

My husband, Kevin, for his support, love, and dinners.

My parents for their encouragement throughout my life, unfailing support, and awesomely smart genes!

All the people who wrote the references in my Bibliography; I am truly "standing on the shoulders of giants."



## TABLE OF CONTENTS

<b>LIST OF TABLES .....</b>	<b>ix</b>
<b>LIST OF FIGURES .....</b>	<b>xi</b>
<b>1 Introduction.....</b>	<b>1</b>
1.1 Atmospheric Stability and Meandering Plumes .....	2
1.2 Gas Density Differences .....	5
1.3 Models .....	7
1.3.1 Gaussian Model .....	8
1.3.2 Non-Gaussian Models.....	10
1.3.3 Problems with Models .....	12
1.3.4 Model Recommendations .....	14
1.4 Previous Experiments .....	16
<b>2 Materials and Methods.....</b>	<b>23</b>
2.1 Previous Experiment.....	23
2.2 Extending on Sawyer’s Experiment .....	27
2.2.1 Making the Continuous Vectors .....	27
2.2.2 Animating the Continuous Vectors.....	28
2.2.3 Performing the Stochastic and Statistical Analyses.....	29
2.2.4 Challenges to My Model Development .....	34
<b>3 Results and Discussion.....</b>	<b>37</b>
3.1 Weather Station Results.....	37

3.2	PID Results .....	39
3.3	Statistical Results .....	42
3.3.1	Fractional Bias (FB).....	42
3.3.2	Geometric Mean Bias (MB).....	43
3.3.3	Normalized Mean Square Error (NMSE) .....	44
3.3.4	Geometric Variance (VG).....	46
3.3.5	General Statistics Remarks .....	47
<b>4</b>	<b>Conclusions.....</b>	<b>49</b>
	<b>REFERENCES.....</b>	<b>51</b>
	<b>Appendix A. Details of Extending Sawyer’s Experiment .....</b>	<b>55</b>
4.1	GMS Analysis.....	55
4.2	SCIPuff Analysis .....	60

## LIST OF TABLES

Table 1.1. Atmospheric Stability Classes (Briggs 1973).....	2
---	---



## LIST OF FIGURES

Figure 2.1. Grid of Photo-Ionization Detectors (PIDs) used in the Experiment. The blue dots represent the PIDs, the red triangle is the release point, or ground zero, and the yellow squares represent the meteorological stations. ....	24
Figure 2.2. Wind Direction over the Ninth Ammonia Release. Note how the wind direction varied between 152.57° and 276.19° for weather stations at heights of 2 meters, which was a span descriptive of most releases. The weather station at a height of 16 meters, Weather Station 10, shows a different wind direction, suggesting that 3-D wind analysis is vital for low wind speed studies. ....	26
Figure 2.3. Wind Speed During the Ninth Ammonia Release. The average wind speed for this release was 2.15 m/s. Other releases were similar wind speeds. ....	26
Figure 2.4. GMS Interpolated 2-D Grid of PIDs with Contaminant Plume Contours. On the left is the logarithmic scale for the PID sample concentrations, in ppm. ....	29
Figure 3.1. (Repeat of Figure 2.2.) Wind Direction over the Ninth Ammonia Release. Note how the wind direction varied between 152.57° and 276.19° for weather stations at heights of 2 meters, which was a span descriptive of most releases. The weather station at a height of 16 meters, Weather Station 10, shows a much different wind direction, suggesting that 2-D wind analysis is not enough for low wind speed studies. ....	38
Figure 3.2. Average Predicted and Observed Concentrations through Time at 50 meters. A good model would envelope both the predicted and observed concentrations within the 6σ range. This suggests the presence of vertical motion in the observed plume, and not in the predicted. ....	41
Figure 3.3. Leveled-Off Fractional Bias (FB) Values of the Ethylene Release #2 at 50 meters. These values were taken at the point where additional statistical releases did not greatly change the value of the FB at each specific time-step. This was accomplished by generating each statistic iteratively throughout the generation phase of this evaluation. ....	43
Figure 3.4. Leveled-Off Geometric Mean Bias (MB) Values of the Ethylene Release #2 at 50 meters. These values were taken at the point where	

additional statistical releases did not greatly change the value of the MB at each time-step. This was accomplished by generating each statistic iteratively throughout the generation phase of this evaluation. The y-axis is log-scale.....44

Figure 3.5. Leveled-Off Normalized Mean Square Error (NMSE) Values of the Ethylene Release #2 at 50 meters. These values were taken at the point where additional statistical releases did not greatly change the value of the NMSE at each time-step. This was accomplished by generating each statistic iteratively throughout the generation phase of this evaluation. The y-axis is log-scale.....45

Figure 3.6. Leveled-Off Geometric Variance (VG) Values of the Ethylene Release #2 at 50 meters. These values were taken at the point where additional statistical releases did not greatly change the value of the VG at each time-step. This was accomplished by generating each statistic iteratively throughout the generation phase of this evaluation. The y-axis is log-scale. ....46

Figure A.1. Example of Excel Data Manipulation for GMS. Each PID was listed by number and location and their concentrations corresponded to times on the upper row. Each observed concentration (in ppm) was placed on its original time and assumed constant until the next measurement was taken; then the pattern repeated. ....57

Figure A.2. GMS Interpolated 2-D Grid of PIDs with Time-Step Window. ....58

Figure A.3. (Repeat of Figure 2.4.) GMS Interpolated 2-D Grid of PIDs with Contaminant Plume Contours. On the left is the logarithmic scale for the PID sample concentrations. ....59

# **1 Introduction**

Low wind speed conditions should be studied because these conditions can present risk because of the high chemical concentrations that can result without being dispersed by higher winds, particularly for areas immediately surrounding the release point. In the case of low wind speed conditions, pollutants do not travel far from the source and the concentration distribution is not cone-shaped, rather, it is non- Gaussian, and often has multiple peaks (Sagendorf and Dickson 1974; Sharan et al. 2003; Sharan and Modani 2005). It is difficult to predict the location and concentration of low wind speed plumes, but there are some proposed methods that can provide approximate answers. The following research attempts to clarify the processes and parameters that govern both the general and low wind speed cases by determining the accuracy and uncertainty of standard prediction methods for low wind speed plume modeling and attempting to determine the causes of modeling errors. This will be done by comparing field-measured experimental data with stochastic model runs. The model runs are designed to evaluate the effects of parameter uncertainties and evaluate this by assuming different parameter distributions for several of the most important modeling parameters.

## 1.1 Atmospheric Stability and Meandering Plumes

One of the most important parameters in chemical plume transport modeling is atmospheric stability. The stability levels are divided into classes, which are dependent on wind speed and whether it is day or night (Briggs 1973). Table 1.1 shows the original Pasquill-Gifford (P-G) stability classification in a simplified manner (Briggs 1973). The time of day and year affect plume characteristics and movement. The atmosphere becomes considerably more stable and therefore more likely to allow high chemical concentrations to occur (potentially hazardous and presenting more risk) during winter periods, which are associated with very stable conditions. These cases are more hazardous because any released chemicals are not readily dispersed in the environment and the plume can continue to have high concentrations, even though it is moving. For example, the infamous Bhopal gas leak occurred during stable winter conditions (Sharan et al. 1995; Sharan and Modani 2005). Summers tend to have more volatile atmospheres which mix and dilute the plume and thus, less frequent conditions for meandering high concentration plumes exist.

**Table 1.1. Atmospheric Stability Classes (Briggs 1973).**

Wind Speed (m/s)	1	2.5	4.5	7
Day	A	B	C	D
Night	F	E	D	D

P-G stability classes range from A to F, very unstable to very stable, respectively. The behavior of plumes in A and B stability classes can be described as looping (Gifford 1975), which is when plumes travel in vertical circles caused by heat-induced eddies. These are normally large eddies that take time to form. This differs from classes C and

D, in which coning occurs (Gifford 1975). Coning is what is typically thought of when a static plume is described. The three-dimensional plume extends outward in a cone-shape, slowly dispersing until the cone's diameter is so wide that the plume is essentially non-existent. In stability categories E and F, a phenomenon known as fanning occurs (Gifford 1975). The fan plume is more two-dimensional than the cone, extending mainly in the horizontal plane. Fans occur during those stability classes that are known for having inversions. An inversion blocks off the upper atmospheres creating a "glass ceiling" for the plumes, thus, causing them to extend outward instead of upward. This reduces mixing and contaminant levels in the plumes can stay high or even build over time.

There is another stability class, which was designated after the original P-G six. It is known as the G class and is even more stable than the F, but with wind speeds of less than 2 m/s (Dobbins 1979). Class G stability normally occurs in near-calm situations, typically on clear nights with frost or heavy dew, and has a diffusion that is appreciably slower than category F (Gifford 1975). Sagendorf suggested that a plume under G stability conditions "meanders" or swings, thus lowering the average concentration in a particular angle wedge to that of about a category C (Gifford 1975). It is essential, when dealing with class G conditions, to have estimates of plume meandering characteristics (Gifford 1975).

Meandering of plumes is an interesting phenomenon. It often occurs close to the source, while the plume is still narrow and relatively concentrated (Hanna 1986), and in strongly stable atmospheric conditions with low wind speeds (Kristensen et al. 1981). The meandering in low wind speeds (below about 2 m/s), has a low-frequency (Oettl et al. 2001) and leisurely pace. A cause for meandering, in both the lateral and vertical

directions, is the spatial distribution of large eddies in the flow (Arya 1999), as mentioned earlier. Another cause might be connected to gravity, which has been found to have periods of five to thirty minutes (Etling 1990).

Two terms are used to describe a meandering plume,  $\sigma_y$  and  $\sigma_z$ , which are measurements of the cross-wind concentrations. Meandering causes  $\sigma_y$  to be dependent on the averaging time (Kristensen et al. 1981). Therefore, an accurate description of  $\sigma_y$  depends upon the time-frame involved and requires normalization if comparisons are to be made. Because meandering is also related to wind speed,  $\sigma_y$  is related to wind speed. It has been found that  $\sigma_y$  becomes small for wind speeds greater than 8 m/s (Kristensen et al. 1981), which implies that  $\sigma_y$  values are relatively large for low wind speed conditions. Larger dispersion values ( $\sigma_y$  and  $\sigma_z$ ) have been found to cause a reduction in long-term concentration levels by a factor of four or more, when compared to straight plume conditions (Etling 1990). ASTM (2000) suggests that the cross-wind concentration distribution (a function of  $\sigma_y$  and  $\sigma_z$ ) is not likely to be Gaussian when wind shifts and concentration fluctuations are taken into consideration (Chang and Hanna 2004). Thus, when a plume meanders, it does not have a Gaussian cross-wind concentration distribution and cannot be modeled as such, which most state-of-the-practice models do.

Two other important parameters are the release height of the contaminant, which is the originating height for the plume, and the duration of release. For ground sources, the highest ground concentrations generally occur at low wind speeds, especially at nighttime (Briggs 1973). This is due to the fact that at low wind speeds the atmospheric conditions are stable and there are little, if any, vertical eddies to bring the plumes away from the ground and cause mixing and dilution. It has also been found that in nocturnal

stable conditions, the power spectra of lateral wind components exhibit two regions with considerable energy. These regions are separated by a gap and can be divided into a high frequency portion due to turbulence and a low frequency portion due to larger scale fluctuations (such as meandering) of the wind direction (Brusasca et al. 1992).

## **1.2 Gas Density Differences**

There are three density classifications of chemicals in the atmosphere; lighter than air (buoyant gases), approximately equal to air (neutral gases), and heavier than air (dense or heavy gases). It is important to note the differences between these classifications and how the gases in each disperse within a plume because each class needs to be modeled differently.

Some buoyant contaminants that have been used in previously performed experiments are sulfur dioxide (Barad 1958), zinc sulfide fluorescent powder, fluorescein, rhodamine B, and krypton-85 (an inert gas) (Nickola 1977).

Dense gas plumes behave as independent, continuous clouds whose physical properties (density, temperature, turbulence level) differ significantly from those of ambient atmosphere and must be treated differently from trace gas or buoyant gas dispersion (Ermak et al. 1989). Some examples of dense gases are liquid nitrogen gas, Freon-12 (in high concentrations), ammonia, nitrogen tetroxide (Ermak et al. 1989), and liquid methane gas (Hanna et al. 1991b). There has been some work done with dense gases, but there remains much that is unknown about their movement. It is important to study these gases because they can be the most dangerous because they tend to move

slowly across the ground in high concentrations, thus increasing exposure time to humans and other living organisms on the ground.

The separation of dense gases and lighter gases is important because there are at least three effects observed in dense gas dispersion that are not seen in trace emissions (Ermak et al. 1989). The first is that the turbulent mixing within the vapor cloud is reduced because of stable stratification of the dense layer in the plume itself. The second is that gravity spreading and self-induced vortices occur because of density gradients in the horizontal direction. The third effect is the fact that cloud lingering occurs when the dense gas cloud travels downwind at a slower rate than the ambient wind speed because of reduced mixing between the dense gas layer and the ambient atmosphere. The first two effects produce lower and significantly wider clouds than trace or neutral density gas releases (Ermak et al. 1989). As the cloud mixes with the surrounding ambient atmosphere, the cloud becomes more dilute, in-cloud properties approach ambient levels, and the previously mentioned effects begin to play a less significant role (Ermak et al. 1989). As long as the dense gas is separate from the air, it behaves as a dense gas. As it dissipates and takes on more of the atmosphere's characteristics, it becomes less like a dense gas and behaves as a trace plume. These effects are the most pronounced when ambient windspeed is low and atmospheric conditions are stable (Ermak et al. 1989), like in the Bhopal gas release.

Dense gases have other odd behaviors. For example, they can bifurcate; leaving the middle of the cloud as a minimum of concentration, not a maximum (Ermak et al. 1989). This makes them quite difficult to model or predict. Clouds can also linger, regardless of ambient windspeed (Ermak et al. 1989). This occurs because the gas settles

to a height not affected by wind, often in a low spot in the terrain. When winds can affect the gases, they disperse faster. Either way, the heavy gas cloud will eventually begin to disperse in a manner similar to a trace gas cloud (Ermak et al. 1989). Once the dense gas is diluted to that point, it can be modeled as a lighter than air gas, but not before then.

Heavy gases are modeled differently than lighter gases. Heavy gas dispersion models are best evaluated by using cloud structure and concentration parameters (Ermak et al. 1989). These parameters include measured plume concentration as function of downwind distance from source, ground level, plume centerline average concentration, plume half-width, and plume height (Ermak et al. 1989). Due to the fact that all the values are steady state, time is essentially irrelevant (Ermak et al. 1989).

### **1.3 Models**

In addition to density, wind speed is an important parameter to use when choosing a model that will correctly predict a plume's path. Chemicals (or gases) downwind of the release in low wind speed conditions may no longer form a cone-shaped plume (Sharan et al. 1996b). Slade (1968) defined eight types of plume behavior: coning, meandering/fanning, looping, lofting, trapping, fumigating, bifurcating, and downwashing (Moore et al. 1988). Each of these types of plume behavior may require a different model to accurately predict the plume shape because most models are developed to predict transport for a given set of conditions.

There are four general types of air quality transport models: Gaussian, numerical, statistical, and physical (Arya 1999). Gaussian models are used for estimating the impact of non-reactive (passive) pollutants from specified point and/or line sources in simple

terrain (Arya 1999). Simple terrain is considered to be any area where the terrain features are lower in elevation than the release height (Arya 1999). This model assumes an ideal world and time-averaged behavior. Numerical models are used for complex terrain and complex flow simulations using point, line, and area sources emitting reactive chemicals on local (urban), regional, and global scales (Arya 1999). These situations have many more variables and are much more difficult to predict, thus requiring numerical analysis to incorporate the spatially varying parameters. Statistical (empirical) models are used in situations where incomplete scientific understanding of physical and chemical processes or lack of required databases render the use of the Gaussian and numerical models impractical (Arya 1999). Physical models use meteorological wind tunnels, convection tanks, or other fluid modeling facilities to simulate the plume. They are used to gain a better understanding of flow and dispersion processes in complex flow and terrain situations (Arya 1999). The results from physical models are used to develop or validate other approaches and models.

### **1.3.1 Gaussian Model**

Gaussian models make many assumptions and approximations (Arya 1999). In general, Gaussian models have limited applicability. They are limited to locations with relatively flat and homogeneous surfaces, winds that are reasonably steady with moderate to strong speeds, atmospheric conditions that are moderately stable to unstable (P-G classifications of A through C or D), gases that are neutrally or slightly buoyant, and relatively short distances (less than 50 km) from simple source configurations (Arya 1999). Gaussian models, like all models, also have large uncertainties due to natural variability and simplified model physics (Arya 1999). Limitations for Gaussian models

arise from the simplifying assumptions used in their formulation, simplified physics, and parameterization of complex turbulence and diffusion processes (Arya 1999).

Some of the more detailed assumptions according to Arya (1999) are:

- 1) Continuous emission from the source at a constant rate, at least for a time equal to or greater than the time of travel to the receptor of interest,
- 2) Steady-state flow and constant meteorological conditions, at least over the time of transport from the source to the farthest receptor,
- 3) Conservation of mass in the plume; nothing is removed and no absorbing boundaries exist,
- 4) Gaussian or reflected-Gaussian distribution of mean concentration in the lateral and vertical directions at any downwind location in the plume (The assumption of Gaussian distribution in the vertical direction is somewhat questionable, but does not appear to adversely affect the model-predicted ground-level concentrations.),
- 5) A constant mean transport wind in the horizontal plane (This implies horizontal homogeneity of flow and the underlying surface, therefore becoming invalid over complex terrain. Thus, the Gaussian model assumes simple terrain.),
- 6) No wind shear in the vertical direction, (The variation of wind direction with height is ignored, although its effect on the lateral plume spread and concentration field can be considered superficially through an appropriate parameterization of  $\sigma_y$ .), and
- 7) Strong enough winds to make turbulent diffusion in the direction of flow negligible in comparison with mean transport. Thus, the Gaussian model limits diffusion in favor for advective transport.

With all the assumptions required to use Gaussian models, it should be obvious that they may not be accurate and should not be used under low wind speed conditions (Arya 1999; Sharan and Modani 2005; Brusasca et al. 1992). In fact, plumes in stable low wind speed conditions can be up to six times more spread out than predicted by Gaussian models (Brusasca et al. 1992). This model failure comes from neglecting downwind diffusion in addition to advection, the lack of appropriate dispersion parameters (Sharan and Modani 2005), and the mathematical assumption that the concentration in the plume approaches infinity as the wind speed approaches zero (Anfossi et al. 1990).

### **1.3.2 Non-Gaussian Models**

When time-averaged to infinity (asymptotically), plume shapes will theoretically be Gaussian in distribution (Gifford 1959), but when predicting an individual plume, Monte Carlo and other numerical methods, are needed to replace the Gaussian models for low wind speeds (Anfossi et al. 1990).

Studies have been done to determine which model is best suited for low wind conditions. Some researchers found that the concentrations near the mean plume axis tend to follow a power law (Gifford 1959). Others developed an ad hoc model based on Gifford's fluctuating plume (1960), which assumes that the total dispersion of the meandering plume is the sum of two contributions: instantaneous diffusion around the plume centerline due to small scale turbulence and dispersion of the instantaneous plume centerline from its time-averaged value due to larger scale wind fluctuations (Brusasca et al. 1992). The Lagrangian method, another approach, uses a "tagged" fluid particle and

follows that particle through time (Arya 1999). This is a method that is modeled using differential calculus and numerical methods. Still others use different numerical methods and different approaches to Fickian diffusion.

Many experiments have used the jackknife and bootstrap sampling procedures for data analysis and to analyze model fit (Tangirala et al. 1992; Cox and Tikvart 1990; Yadav and Sharan 1996). Jackknifing is the most efficient procedure to apply (a few seconds of computer time compared to the fifteen minutes needed for the bootstrap method [on an IBM PC/AT]), but jackknifing has slightly overestimated confidence bounds (Hanna 1989). It should, therefore, only be used for means or variances (Hanna 1989). The Bootstrap method uses a new set of 'N' values of the difference between the predicted and observed concentrations ( $C_p - C_o$ ) randomly drawn from the original set. If a given ( $C_p - C_o$ ) is drawn, it is replaced before the next draw is made, thus, it is possible that all 'N' draws consist of the same value of ( $C_p - C_o$ ). For each re-sampled set of size 'N,' the mean-square error (MSE) is calculated for all ( $C_p - C_o$ ) values. This provides confidence limits on the MSE (Hanna 1989). Bootstrapping, unfortunately, also causes erroneous conclusions at the tails of the distribution function (Hanna 1989).

Another non-Gaussian method is K-Theory. The constant K-Theory method is a model that uses Fickian diffusion (Arya 1999). Constants can be found by parameterizing the vertical turbulence and diffusion in the surface layer using local free convection similarity theory (Sharan et al. 1996b). The variable K-Theory approach is based on power-law profiles for wind speed. One of the variables,  $K_z$ , has been suggested as an alternative to the Gaussian model (Arya 1999).

### 1.3.3 Problems with Models

As with any model, plume transport models have uncertainties associated with predictions. One of the problems with models is that they may appear quite accurate during validation and calibration when actually one error is canceling another (Ermak et al. 1989). The Gaussian model overestimates low wind condition characteristics (Sharan et al. 1996a). What complicates the results further is that the model changes when plume parameters are defined in a particular way (Ermak et al. 1989). A complication with many models is that constant eddy diffusivity for near-source dispersion cannot be assumed (Sharan et al. 2002). It is also difficult to simulate plume directions in wedges of twenty to forty degrees, and thus, the observed and predicted contours seldom overlap (Chang and Hanna 2004).

Often physical factors in plume transport are not understood. This is illustrated by the fact that in two out of three of Hanna's data groups; the "best" model was found to be one that was not originally developed for that scenario (Hanna et al. 1991b). When a model is being developed, extra and/or new dimensionless constants should not be allowed to slip into the model. These should be avoided because if they are required, they represent factors in the model that cannot be fully explained or understood at the present (Briggs 1975).

Some factors are not normally accounted for in plume models due to their extreme application difficulty. One somewhat elusive problem is how to account for gravity waves in the wind fluctuations (Brusasca et al. 1992). This is a small influence, but in low wind speed conditions, it can be important. Another phenomenon often not accounted for in models is particle settling. When taken into consideration, the particle

settling velocity may decrease the concentration throughout the plume (Gifford 1975). Another issue with particle settling is that particles can be re-suspended into the plume (Gifford 1975). This occurs because washout (or particle settling) is a reversible process that does not change the shape of the plume (Gifford 1975). A third difficulty occurs when modeling cities. This is because they are more complicated with their mechanical and thermal heat, as well as, a greater surface roughness. Air flow in city models is much more turbulent than open land (Gifford 1975).

Two main particular difficulties occur during simulation of low wind speed situations. The first is that low wind speed plumes are generally associated with strong stability and air stagnation, which correspond to highly non-stationary and inhomogeneous diffusion processes. Low wind speeds also cause “puddling,” or air stagnation, (Brusasca et al. 1992) which is difficult to predict and model. The second is the fact that dispersion is dominated by the fluctuations in wind direction (which can be quite large compared to the main component of transportation in the mean direction), or meandering under these conditions (Anfossi et al. 1990).

In low wind speed conditions, a model cannot assume that the pollutants are transported in the mean direction at the mean wind speed or dispersed by turbulence. Neither can the model assume that the diffusion along the mean wind direction is negligible in comparison to the transport (Brusasca et al. 1992). This rules out Gaussian models and demands a detailed inclusion of diffusion. Also, due to crosswind spread, the measured concentrations at ground sources may appear lower than calculated (Van der Hoven 1976). This causes models validated against measured results to be conservative,

which is not a problem when evaluating risk, but should be noted when making best estimate predictions.

At the International Meeting at Torino University on Dispersion in low wind speeds and foggy conditions; organized by the European Association for the Science of Air Pollution (Anfossi et al. 1990), they concluded that not enough was known and thus, more effort should be spent in this field (Brusasca et al. 1992). This does not provide encouragement for accurate use of current models for low wind speed conditions.

The most important item to remember when choosing models for low wind speed conditions is to check the assumptions (Oetl et al. 2001). Two important assumptions are a homogenous wind field and restrictions on the shape of the source. These cause models to have limitations whenever the chosen time intervals are below the ratio of the maximum travel distance to the average wind speed ( $x_{\max} * \sqrt{u}$ ), where  $x$  is the maximum travel distance and  $u$  is the average wind speed (Oetl et al. 2001). When testing models with experimental datasets, it is currently difficult to find a more severe dataset than the INEL dataset (Brusasca et al. 1992) to challenge a model under these conditions.

#### **1.3.4 Model Recommendations**

When preparing to analyze data using a model, it is important to consider a few items before selecting a model. First and foremost should be the applicability of the model to the scenario of interest and the model's stability. The resources required to implement the model should also be analyzed. Is the model of interest for the expected use of the study; both current and subsequent requirements? What is the overall cost of the model; in money, time, and resources? Is a newer, or older, type of computer

required to run the model? Is there an available user's guide and/or technical description that can be accessed easily? Is the source code for the model, or the developers, available if needed for clarification? Another vital issue is the ability to meet the model's input data requirements. Do all variables have measured values or were the values made to fit the data that was gathered? Additionally, are the output data in the format required for the analysis? (Hanna et al. 1991a).

Models of atmospheric transport and dispersion must incorporate knowledge of at least four parameters (Sugiyama et al. 2003). These include first the physical properties of the airborne material and the release mechanism; second the geometry, if there is a time varying release rate, and other dynamic processes. Third, are the complex meteorological conditions (including spatial and temporal variations) and, fourth, the characteristics of the terrain and structures surrounding the release location (Sugiyama et al. 2003).

It is important to calibrate the chosen model with a situation similar to your experiment (Hanna et al. 1991a). If possible, the model should be calibrated with data from a third party. If a Gaussian plume model does not fit the data, it may be necessary to modify that model to accurately predict the plume (Etling 1990) or use a diffusion model with the actual distribution (Hanna 1983).

Each experimental situation has limitations. Thus, all empirical equations need to be evaluated for each stability level and wind condition because they are non-transferable between them (Sharan and Yadav 1998). The experimental set-up also influences the limitations of the study. Chang and Hanna (2004) claim that

*“... the monitoring instruments for short-range dispersion field experiments are typically arranged in concentric arcs. The data from*

*these arcs are adequate to measure the plume's cross-wind distribution, but are usually insufficient to plot contours. This is especially so if the number of sampling arcs is limited. And in the case of routine air quality monitoring networks, the ten or so monitors are generally scattered around at various angles and distances, and any contours that may be attempted would be highly uncertain."*

When researchers are concerned with regulatory requirements, they often use the centerline concentration to assess model performance (Chang and Hanna 2004). This provides a conservative assessment due to the fact that the concentration is generally higher at the centerline than elsewhere in the plume. If a dense collection of monitors was set up for a long period of time, it is possible that this centerline estimation might be bypassed due to a more complete knowledge of plume movement.

#### **1.4 Previous Experiments**

Theoretical and experimental work take different approaches to solving the same problem. Theoretical work usually starts by analyzing simpler situations and then increasing the complexity. With plume modeling, the theoretical work begins with instantaneous source diffusion, which then grows to a small puff, and then proceeds by integration to other sources, such as continuous or line. This is a very different approach to experimental work because the latter usually starts analysis of a continuous point source. There are three main reasons for this tendency (Barad 1958). The first reason is that engineering a continuous source with reproducible characteristics is generally simpler than a puff source. The second is that the statistical interpretation of concentration measurements from a constant source at downwind stations is simpler than a situation that requires analysis of instantaneous diffusion from a puff source. And the third reason is that the determination of what constitutes pertinent meteorological data

and the provision of such are generally simpler for a continuous plume where time averages can be used (Barad 1958).

There are different methods for testing how much contaminant was detected at each point in the experiment. Before Photo-Ionization Detectors (PIDs) were available, scientists needed to be creative with detection methods. One such method, developed by the Massachusetts Institute of Technology (MIT), was specific to sulfur dioxide releases. It involved filling receptors with hydrogen peroxide and then measuring the amount of sulfuric acid in the receptors after the test (Barad 1958).

Some examples of continuous passive gas releases include projects Prairie Grass, Green Glow, Dry Gulch, Ocean Breeze, Green Glow, Sandstorm, Adobe (Hanna et al. 1991a), and the 67-Series (Nickola 1977).

Project Prairie Grass was conducted at O'Neill, Nebraska in 1956 with neutrally buoyant passive tracers, specifically sulfur dioxide, and with 60 scientists, technicians, and test support personnel (Barad 1958; Arya 1999). It involved MIT, Texas A&M Research Foundation, University of Washington, University of Wisconsin, Air Weather Service, and units of the Air Force Cambridge Research Center (Barad 1958). The experiment's purpose was to determine the rate of diffusion of a tracer gas over 800 meters, as a function of meteorological conditions (Barad 1958).

The tests occurred in a large, flat field in the Great Plains and consisted of about seventy continuous releases of ten minute durations at a height of a half meter above the grass surface (Barad 1958; Arya 1999). Six of these releases occurred in wind speeds of less than 2 m/s, but only four are complete tests with valid data (Barad 1958). It is interesting to point out the rationale for the ten minute releases. It was a compromise of

the cost of the tracer gas, practical rates of emission, distance between samplers, and the desire to have a fairly stable time-mean diffusion pattern in the downwind area (Barad 1958). Concentrations were measured at one and a half meters above the ground in semicircular arcs at various distances between 50 and 800 meters from the source. Vertical concentration distributions were also measured from six 20-meter towers mounted along the 100 meter arc (Barad 1958; Haugen 1959; Arya 1999).

An experiment similar, and prior to, Prairie Grass took place at Round Hill Field Station at MIT, which was a rougher and uneven site (Barad 1958; Cramer et al. 1958; Arya 1999). This was to test indication methods and it was found that flatter land was needed to perform the experiment successfully. An entire square mile was desired to collect samples over greater downwind distances and over more uniform terrain and vegetation (Barad 1958), thus, Project Prairie Grass was conducted.

Project Prairie Grass filled in the gap for diffusion data where the Great Plains Turbulence Field Program failed. Participants in the latter were prepared to make a variety of meteorological measurements, but neither were prepared to make quantitative diffusion measurements. Neither series had both a satisfactory tracer technique and the equipment needed to collect tracer samples in a dense network of stations (Barad 1958).

Project Green Glow at Hanford, Washington, was a series of 76 diffusion experiments in 1959 (Nickola 1977). Zinc sulfide was released at one and a half meters above the ground and concentrations were measured on arcs between 200 m and 25.6 km from the source. Vertical concentration profiles, up to heights of 62 meters, were measured at a number of towers. The terrain for the experiments was quite flat to gently rolling with sagebrush cover one to two meters high. The tracer was released for 30

minute periods through two fog generators and the fluorescent particles collected on the filters (Fuquay et al. 1964; Arya 1999).

Another experiment at Hanford was the 67-Series, called such because they happened after July of 1967 (and before 1973) (Nickola 1977). Almost all of the 103 tracer releases lasted 30 minutes and all were completed in 54 nonconsecutive days (Nickola 1977). Often, multiple tracers were released simultaneously from different heights, ranging from ground level to 111 meters high (Nickola 1977). Up to 718 field locations within 3.2 km of the release site were used for tracer concentration sampling during each release and each sampling point was between one and a half and 62 meters up. The sampling apparatuses were membrane filters and Geiger-Müller tubes (Nickola 1977). This experiment was useful in determining general plume movement, but did not focus on low wind speed conditions.

Other experiments were located at Cape Canaveral, Florida, Vandenberg Air Force Base, California, and Idaho Falls, Idaho (Arya 1999). The National Reactor Testing Station in Idaho Falls performed experiments during unstable atmospheric conditions with uranin dye in a solution. The solution was released 46 meters above the ground and the mean concentrations were measured along six arcs of ground samplers extending from 150 to 1800 meters from the release point. It was found that the vertical and lateral plume spreads were proportional to standard deviations of wind direction fluctuations (Arya 1999).

In an experiment specifically designed for wind speeds less than 2 m/s, Cirillo and Poli (1992) implemented a full 360° sampling grid with arcs at 100, 200, and 400 meters out, at every 6° of the circle. This set-up was designed to compensate for the wind

direction variability. This experiment gave almost identical results for Sharan and Yadav (1998) using the Idaho National Engineering Laboratory (INEL) dataset from 1974 (Oetl et al. 2001). It is interesting to note that these two experiments were performed in completely different parts of the world (Brusasca et al. 1992) and still had very similar outcomes.

The INEL test was conducted in the southeastern portion of Idaho, on a flat, semi-desert plane at an elevation of about 1500 meters above sea level (Brusasca et al. 1992). Sulfur hexafluoride was released at a height of one and a half meters while a cloud of oil fog was emitted simultaneously in order to allow a visual observation of the plume path (Brusasca et al. 1992). One of the criteria for the INEL tests were wind speeds lower than 2 m/s and ten of the 11 tests performed met that criteria (Brusasca et al. 1992). To achieve the wind speeds desired, the tests were performed during night or early morning (Brusasca et al. 1992). The tests were one hour long and the one hour average tracer concentrations were observed on three circles with radii of 100, 200, and 400 meters (Brusasca et al. 1992). Each circle had 60 samplers, each 0.76 meters tall, at intervals of 6° (Brusasca et al. 1992).

In addition to the passive tracer releases, dense gases have also been studied. Some examples of experiments that released dense gases include Burro, Coyote, Desert Tortoise, Eagle, Falcon, Goldfish, Maplin Sands, and Thorney Island-C (Hanna et al 1991b). These tests were performed in both North America and Europe by various entities. Those with animal names were tests by Lawrence Livermore National Laboratory (LLNL) at the Nevada Test Site. Shell Research Ltd performed the Maplin Sands experiment and the British Health and Safety Executive, Thorney Island (Ermak et

al. 1989). The Burro series investigated heavy gas dispersion by releasing liquid nitrogen gas (Ermak et al. 1989). The Coyote series studied rapid-phase change and combustion phenomena and heavy gas dispersion with the releases of liquid nitrogen gas and liquid methane gas (Ermak et al. 1989). Though these experiments are listed here, when compared to tracer gas studies, there is a dearth of dense gas studies (Ermak et al. 1989).



## **2 Materials and Methods**

Multiple techniques were utilized to incorporate data previously gathered for a different purpose, to generate parameter distributions that could be used to develop stochastic models for chemical plume prediction.

### **2.1 Previous Experiment**

The data used in this analysis were taken during a multi-day experiment performed on Frenchman Flats, a flat, dry lakebed, at the Nevada Test Site (NTS) in February of 2007. The purpose of the conducted experiment was to test the concentration of released contaminants at certain distances and evaluate them with special regard to safety precautions at NTS. The experiment from which these data were taken is explained in detail in Sawyer (2007). I have taken these data and expanded their use to include an analysis of stochastic model prediction of a chemical plume.

The data collected during this experiment included weather data and chemical concentrations throughout the chemical release time. Wind direction and speed data were taken at regular intervals along with other meteorological data, such as solar radiation and atmospheric pressure, by 2-D and 3-D anemometers on weather towers. Four wind sensors were located along the outer sampling ring and one was co-located with the release source at ground zero. There were four other meteorological stations which were

located 20 meters outside the 100 meter ring, on the 45-, 135-, 225-, and 315-lines. The circular grid of PIDs, shown in Figure 2.1, took chemical concentration measurements every few seconds, which were measured in parts per million (ppm).

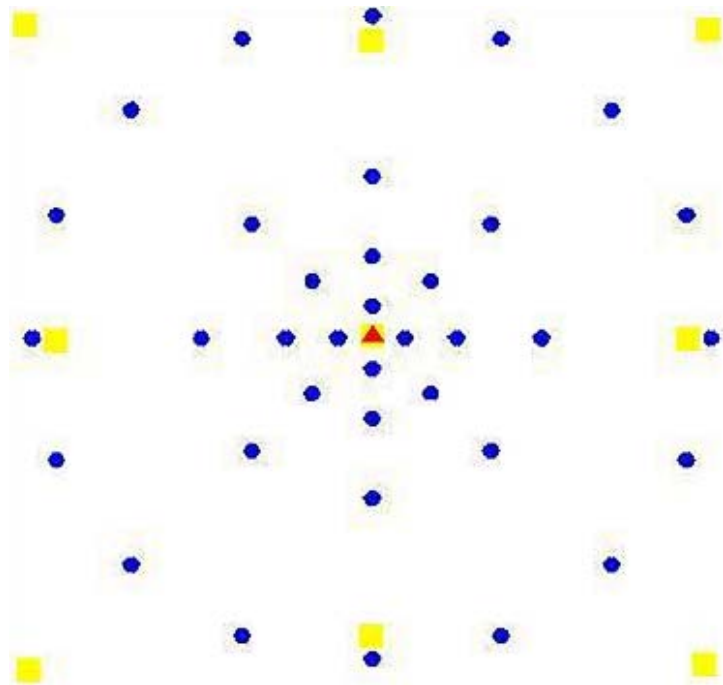


**Figure 2.1. Grid of Photo-Ionization Detectors (PIDs) used in the Experiment. The blue dots represent the PIDs, the red triangle is the release point, or ground zero, and the yellow squares represent the meteorological stations.**

There were 36 PIDs used in the experiment, each set at a height of two meters. This was to measure the concentration at the height of the average man and thus, obtain a relatively accurate measure of what a man would be exposed to during a release of this kind. This height is also important for my analysis because it is high enough that the roughness associated with the ground is negligible and a simpler model can be used for plume prediction.

This was not the ideal setup for my analysis, but was sufficient to achieve results, even if data collection was on a sparser spatial level than desired. The ideal setup for my

analysis would have been a dense wedge of PIDs covering  $60^\circ$  that extended from the release point, up the 225-line, and to a distance of 100 meters. Because this setup was not possible due to the ownership of the experiment, I adapted my analysis to the sparser array.

In order to release the contaminant for the experiments, certain conditions were required to be met. The first was low wind speeds, between zero and two meters per second, were needed to ensure the most unpredictable situation, which would also be the worst case scenario for safety measurements. It was also preferred that the wind be coming up the 225-line, which is from the Southwest to the Northeast. This matched the alignment of the PIDs and also is the dominant direction for wind on Frenchman Flats. For the most part, these conditions were achieved during average test times of 15.08 minutes. Sample graphs of how the wind direction and velocity fluctuated can be found in Figure 2.2 and Figure 2.3.

I used and statistically varied other data taken in the experiment, such as the mass of contaminant released during a release time and release height. These, along with other observed values, were statistically varied so that a stochastic model could be formed and analyzed. The parameters that I varied were varied according to statistical distributions calculated from the measured data.

### Wind Direction for NH3 Release #9

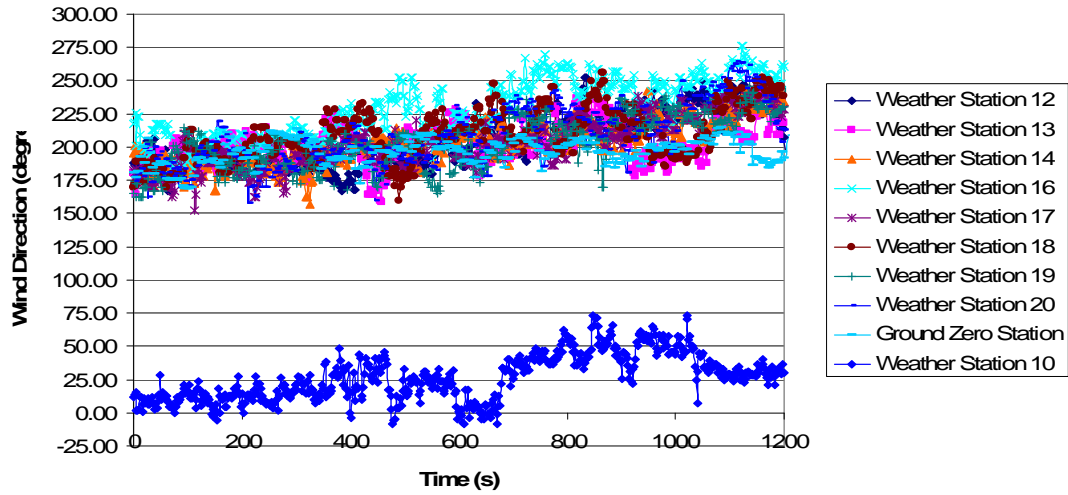


Figure 2.2. Wind Direction over the Ninth Ammonia Release. Note how the wind direction varied between  $152.57^\circ$  and  $276.19^\circ$  for weather stations at heights of 2 meters, which was a span descriptive of most releases. The weather station at a height of 16 meters, Weather Station 10, shows a different wind direction, suggesting that 3-D wind analysis is vital for low wind speed studies.

### Wind Speed for NH3 Release #9

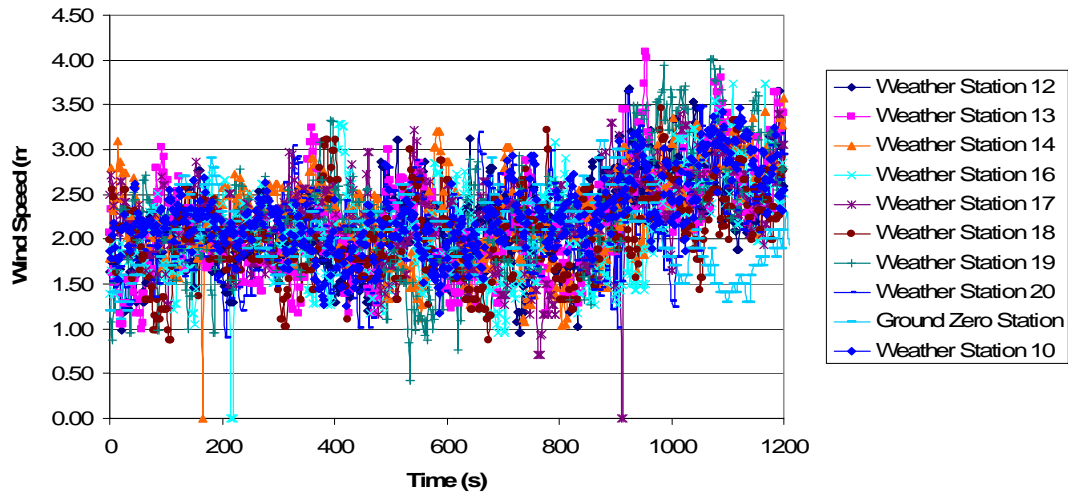


Figure 2.3. Wind Speed During the Ninth Ammonia Release. The average wind speed for this release was 2.15 m/s. Other releases were similar wind speeds.

## **2.2 Extending on Sawyer's Experiment**

I organized the data gathered by Sawyer (2007) into a continuous time series for each sampling location, which were represented as vectors to facilitate the statistical and mathematical analysis. I then animated these vectors with respect to time and performed a stochastic analysis on these observed vectors. Predicted vectors were compared to the observed vectors and a statistical analysis was performed on the results of the comparison of the stochastic process with the observed results. More details as to how these steps were accomplished may be found in Appendix A.

### **2.2.1 Making the Continuous Vectors**

The first step in extending Sawyer's experiment was to turn the discontinuous and erratic time and chemical measurements into continuous interpolated measurements that could be analyzed by pre-existing computer programs. This was accomplished by writing computer programs and manually manipulating the data.

In summary, the first step was to increase the temporal resolution of the time vectors to one second intervals, from the four through eight second intervals in which they were originally collected. Next, the concentration measurements associated with each time were expanded using a stair-step pattern; beginning at the recorded time and continuing until the next recorded time and concentration, the concentration would be the same. Other approaches were considered, such as distance weighted averaging or continuous splines, but these more advanced interpolation techniques could not be justified for these data. This temporal interpolation was done for each of the 36 PIDs' measurement locations in each of the 32 release sequences.

The details of the above mentioned manipulations are explained below. A program I wrote, called “Pull2Cols,” extracted the time and concentration vectors for each PID in each sequence, and saved them in a \*.csv file. I then formatted each \*.csv file by hand in Excel. This was accomplished by transposing the vectors, expanding the \*.csv file into multiple \*.csv files if needed, adding the PID locations, x- and y-coordinates, and stair-stepping the concentrations.

### **2.2.2 Animating the Continuous Vectors**

The finished \*.csv files, with one second data, were then imported into a program developed by the Environmental Modeling Research Laboratory (EMRL) at Brigham Young University (BYU) called GMS (Jones 1998). Inside GMS, the concentrations measured at the PID locations were interpolated to a 2-D grid using the Natural Neighbors interpolation scheme using a Constant nodal function with extrapolation beyond the convex hull. This interpolation scheme avoided the imaginary “peanut” shapes and “zero-hit” voids that appeared when using other interpolation schemes.

Once the grid values were calculated, the contours were developed with values chosen on a log scale. This allowed different concentrations of the contaminant to be visualized on the PID grid. Each contour collection was unique to its time-step for the portion of the \*.csv file within the specific sequence. Thus, when the entire sequence was animated in time, using GMS’s animate function, the contours could be seen to change with each time-step. An example of a 2-D grid with contours for one time-step is shown in Figure 2.4.



for the specific sequence. ‘SMPrun’ called ‘GenStatVars,’ SCIPuff, and ‘Statistics.m’ to perform the entire set of stochastic model runs and subsequent statistical analysis.

### **‘GenStatVars’**

The file ‘GenStatVars’ was where the statistical values for the chosen SCIPuff variables were selected based on the statistical distribution models for each parameter. The variables chosen to be represented stochastically were the vertical and horizontal dispersion coefficients,  $\sigma_z$  and  $\sigma_y$ , respectively, the wind speed, the amount of mass released in the plume simulation (CMASS), the release height, and the time-step, delta. The dispersion coefficients were determined by looking at the Pasquill-Gifford-Turner (PGT) charts for dispersion coefficients as a function of atmospheric stability category and downwind distance (LaGrega et al. 2001). The wind speed was determined by taking a value from the Gaussian distribution created by centering the function over the average observed wind speed and using the calculated standard deviation for the contaminant release. This is shown below.

```
#Wind Speed
#Use avg wind speed for that sequence as found in measured results
#Gaussian, centered over the average of the sequence
stdev= #value of the Std. dev unique to that seq. from measured data
SeqWS= #avg wind speed of sequence being run
WindSpeed=normal_rnd(SeqWS,stdev) #randomly generated value between 0 and 1
```

The CMASS was generated by taking a percentage of the actual release mass with a uniform distribution between  $\pm 10\%$  of the actual mass released. The code used for this variable generation is shown below.

```
#CMASS
#+ or - 10% of what Pat Sawyer had; changes for each sequence
#Random number to give an even distribution for + or - 10% of each seq.
#see CMASS.xls for values for each sequence (use kg of CMASS)
PatValue= #manual updates per sequence
CMASS=(rand()*(0.2*PatValue))+(0.9*PatValue);
```

The release height was set to two meters and the time-step was set at one second. This was the actual release height and a convenient time-step that allowed the desired level of detail to be examined.

These generated variables were saved into a file which ‘SMRun’ extracted and then placed each variable into the corresponding location for the SCIPuff input files. Thus, a single input file with specified blanks could be used for each run because the necessary information was altered for each run. This input file gives SCIPuff all the necessary information to run the plume prediction model.

### ***SCIPuff***

The Second-order Closure Integrated Puff (SCIPuff) model is a Lagrangian transport and diffusion model that can model atmospheric dispersion in a wide range of applications (Sykes 1998). It

*“uses a collection of Gaussian puffs to represent an arbitrary [3-D], time-dependent concentration field, and incorporates an efficient scheme for splitting and merging puffs... The model also uses several types of meteorological input... [and] is appropriate for modeling both short and long range transport, steady or non-steady state emissions of primary pollutants (in the form of gases or particles), [and] buoyant or neutral sources...” (Sykes 1998)*

SCIPuff was developed by the Titan Corporation in Princeton, New Jersey, under the direction of Ian Sykes (Sykes 1998). The Technical Documentation for SCIPuff (Sykes 1998) is recommended for a further and more detailed look at SCIPuff.

In my analysis, SCIPuff was used to calculate model results for all the stochastic sequence runs and create an output file that was then used by ‘Statistics.m.’ This output file consisted of time, concentration, and other vectors through time for each circle of PIDs. I configured SCIPuff to only output information for the centerline of the plume, which has the highest concentration at the location of the four PID ring distances. These PIDs used for the comparison were those that register the highest concentration for that time-step in their distance-circle in the PID array. Thus, there are concentration results for the 10, 25, 50, and 100 meter rings of PIDs at each time step. These were the measured results that were compared with model runs. As with the model, the highest observed PID reading for a given time-step was chosen as the center of the plume (as described above).

### ***‘Statistics.m’***

‘Statistics.m’ is the program I wrote to compute the statistical comparisons between the modeled and observed results. The first step to allow ‘Statistics.m’ to run was to create files containing the observed data. Thus, the centerline plume for each time-step in each sequence was created and saved in a \*.csv file. These data are then compared to the SCIPuff-predicted results throughout ‘Statistics.m.’

Statistical analyses were performed on the observed and model predicted data in accordance with Chang and Hanna’s (2004) paper, *Air quality model performance evaluation*. The SCIPuff model was run stochastically with selected model parameters from the established statistical distributions. After each model run, the model results were compared with the observed results. This was done incrementally, so that I could evaluate how the statistics changed with the increasing number of stochastic runs. I

expected that early, when each individual run significantly influenced the results, the statistical measurements would show large variability. I expected that later, as each individual run had less influence, that the statistical measure would approach a constant value, which would be descriptive of the entire set of stochastic model runs. This turned out to be mostly true.

One of the goals was to determine how sensitive these statistical measures are to varying model conditions within the expected uncertainty for the selected parameters. Each statistical variable was implemented as a matrix to ensure the statistics leveled off and that enough runs were performed to make the model stochastic. The newest column in the matrix represents the results of the last stochastic run of the sequence, and as noted above, the statistics were updated after each run. The continuous updates allowed the statistics to be plotted against the runs thus, showing when they leveled off. This is shown and discussed in the Results and Discussion portion below.

The following statistics were measured: Fractional Bias (FB), Geometric Mean Bias (MB), Normalized Mean Square Error (NMSE), and the Geometric Variance (VG). A perfect model would have values of one for MG and VG and values of zero for FB and NMSE. Equations for these statistics are found in Equations 2.1-2.4 below (Chang and Hanna 2004).

$$FB = \frac{(C_o - \overline{C_p})}{0.5(C_o + \overline{C_p})} \quad (2.1)$$

$$MB = e^{(\ln \overline{C_o} - \ln \overline{C_p})} \quad (2.2)$$

$$NMSE = \frac{\overline{(C_o - C_p)^2}}{C_o * C_p} \quad (2.3)$$

$$VG = e^{\overline{(\ln C_o - \ln C_p)^2}} \quad (2.4)$$

These equations were modified to analyze the stochastic goodness of fit through time due to variable wind speed and direction. The equations were originally developed for time-averaged data collection systems, such as acid neutralization, particle collectors, etc. (Barad 1958; Arya 1999; Chang and Hanna 2004), and Sawyer's (2007) experiment collected instantaneous readings of concentration. I modified the equations to calculate the model fit at each time step.

#### 2.2.4 Challenges to My Model Development

One of the challenges associated with 'Statistics.m' was due to the fact that zero is a valid measurement in the experiment, but is not valid in some of the statistics, specifically the inner mathematical steps involving natural logs and the NMSE.

The natural logs posed a problem because the natural log of zero is equal to negative infinity ( $\ln(0) = -\infty$ ). This, in and of itself would not have been a problem, but the statistics were being developed incrementally, which meant that during each run the current run vector was solved for and its value was equal to the current value plus the value in the last intermediate statistics column. Thus, negative infinity ( $-\infty$ ) plus a small (or large number, for that matter) was still equal to negative infinity ( $-\infty$ ). Regardless of the value of the observed or predicted concentration, the statistics that had a natural log function in them were repeatedly equal to negative infinity ( $-\infty$ ).

The NMSE provided a “division by zero” challenge. When the average measured concentration was greater than zero, NMSE could be solved for without a problem. However, when the average measured concentration was equal to zero, the denominator of NMSE was also equal to zero and NMSE was equal to infinity ( $\infty$ ). This value of infinity ( $\infty$ ) was not wrong, per say, but to implement these equations so that the statistical value could be updated for each stochastic run, it had to be changed.

These issues were solved by declaring all zero values of the observed and predicted vectors to be equal to  $10^{-20}$ . This allows the computer to calculate the statistics for any conditions, including values of zero. This is acceptable due to the fact that a measured value of zero is actually equal to some value between zero and the minimum measuring limit of the equipment.

The final statistical values were then analyzed for their accuracy and to determine how close the predicted models were to the observed. This involved looking at how close each of the statistics was to their “perfect model” values, as mentioned above.



### **3 Results and Discussion**

Ethylene, ammonia, and propylene were released in Sawyer's (2007) experiment. For matters of brevity only a representative example of calculations made for the 32 releases, the second ethylene release, statistical results will be discussed in the following portion of this report. Wind direction insight will also be discussed.

#### **3.1 Weather Station Results**

A surprising result of this analysis is that 2-D wind data in low wind speed plume studies is insufficient for an accurate analysis of the plume. Both wind direction and speed data should be gathered to allow the researcher to build a true picture of what is actually occurring in the experiment.

Data suggest 3-D wind direction data is important for building a clearer understanding of the surrounding environment of the chemical plume. In Sawyer's (2007) experiment, weather stations were placed at 2 and 16 meters above the ground. This allowed more of a 3-D picture to be taken of the volume of air the plume was moving through during the release. As shown in Figure 3.1, the weather stations at a height of two meters record wind directions between  $150^{\circ}$  and  $275^{\circ}$  and Weather Station 10, at a height of 16 meters, records wind directions between  $-10^{\circ}$  and  $75^{\circ}$ . This points to an important fact unique to low wind speed conditions; one should not ignore the third

dimension. In higher wind speeds, lateral advection dominates all other movements, thus horizontal and vertical diffusion and advection can be ignored or lumped together with the diffusion coefficient (Nepf 2006). This was not the case in low wind speed conditions that occurred during these tests, which makes sense because the horizontal and lateral movements decrease in magnitude and the vertical may not change at all. Thus, the relative magnitudes of the vertical movements, as compared to the horizontal and lateral, are larger in low wind speed conditions.

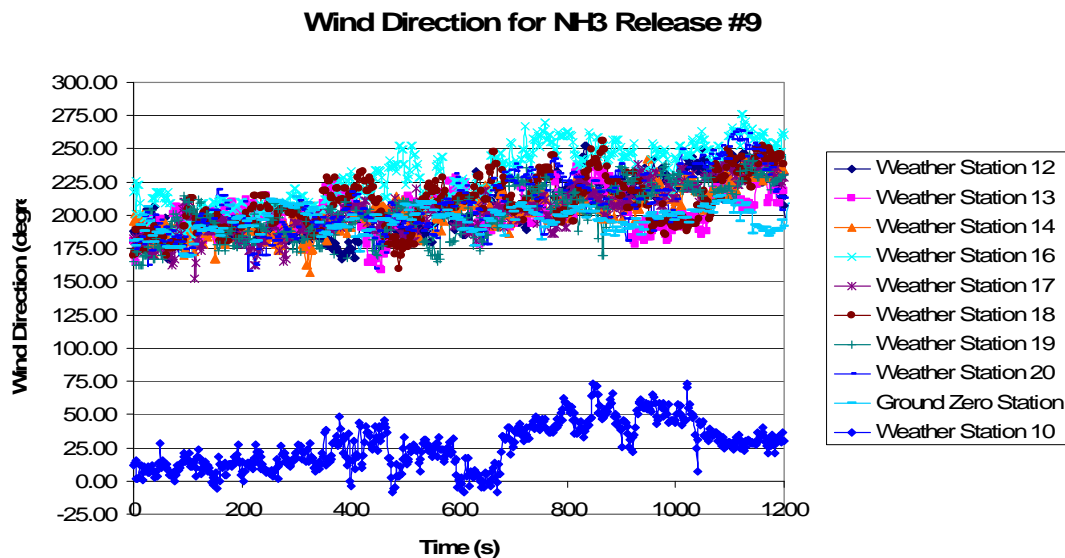


**Figure 3.1. (Repeat of Figure 2.2.) Wind Direction over the Ninth Ammonia Release. Note how the wind direction varied between 152.57° and 276.19° for weather stations at heights of 2 meters, which was a span descriptive of most releases. The weather station at a height of 16 meters, Weather Station 10, shows a much different wind direction, suggesting that 2-D wind analysis is not enough for low wind speed studies.**

We can therefore suggest that further low wind speed studies include 3-D weather stations that measure both horizontal and vertical wind speed to model air movement accurately. An increase in understanding about how air is moving at low wind speeds will aid in understanding and possibly predicting how contaminants in the air move at the

same low wind speeds. This is particularly important when studying movements above a non-flat or non-homogeneous surface.

### **3.2 PID Results**

It is interesting to note that the observed concentrations appear to be clouds or puffs of contaminant traveling through the air. As a contaminant puff approaches the sensors, the detected concentration increases rapidly. The opposite is true for the retreat of the puff. These data show this process due to the instantaneous nature of PID sampling. The five spikes shown in Figure 3.2, specifically between the times of 30 and 37 seconds, 57 and 60 seconds, 83 and 92 seconds, 127 and 142 seconds, and 153 and 176 seconds, clearly delineate the presence of puffs or a looping plume touching the ground. It is unknown if any combination of these puffs are the same puff, brought back around by large eddy motions mentioned above. Another possible explanation is that the released contaminants were caught by different wind gusts and thus, after the plume was split into various puffs, they arrived at 50 meters out at different times. A third explanation concerns the spacing of PIDs in the detection array. It is quite possible that the plume traveled above, below, or directly between two PIDs and they only detected the plume when the edge “got caught” on the PID. If a denser array of PIDs had been available, this question might be answerable. As it is, further study will need to be done to determine if the plume actually split into puffs or if it simply meandered between the PIDs throughout the length of the release.

It should also be mentioned again that the observed concentrations are actually values taken from the centerline analysis of the plume. Thus, the highest concentration

hits achieved during the release are all modeled as if they were in the same direction. Therefore, these puffs could represent five different portions of the plume that split into puffs and traveled in different directions. Any horizontal movement, even if followed by lateral motion, would increase the path time for the puff and cause it to reach a certain distance, in this case 50 meters, at later times.

It was hoped that SCIPuff would create a model that could predict plume concentrations in low wind speeds and that by varying the various parameters in a series of stochastic runs, we could bound the problem. This would create an envelope of concentrations from the model that would predict the observed concentrations with some uncertainty, e.g.  $\pm 3\sigma$ . The graph in Figure 3.2 shows that the  $6\sigma$  envelope does not do a particularly good job of confining the observed concentrations. There are a few observed data points that lay inside the envelope, but only at the fronts and backs of the puffs where the concentrations are expected to be less. Also, most of the points that lie outside the envelope only do so by approximately an order of magnitude, but one of the observed points reaches almost a difference of five orders of magnitude.

Part of this failure of containment is due to the smearing of the concentration with time. The input for this model is time-smearred, as described in Appendix A, thus the mass of modeled contaminants released is over a longer period than in the observed experiments. The model also handles the release as a stream of puffs, not a few smaller, highly concentrated puffs as shown in Figure 3.2. The concentrated values shown by the observed puffs are smoothed over the entire release period in the predicted model; there is no major difference in mass released, only in how it travels after release. This can be seen by the leveling-out of the predicted average concentration; after the first three puffs

pass, the concentration difference between times goes to zero. This suggests that the predicted plume does not leave, i.e. the concentration does not decrease, with the passing of time.

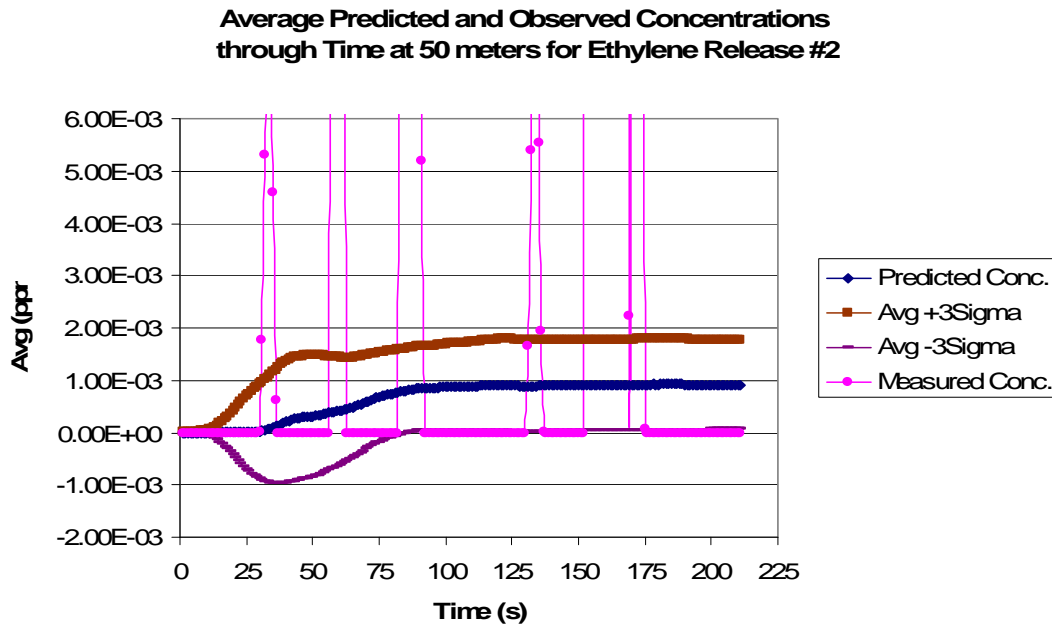


**Figure 3.2. Average Predicted and Observed Concentrations through Time at 50 meters. A good model would envelope both the predicted and observed concentrations within the  $6\sigma$  range. This suggests the presence of vertical motion in the observed plume, and not in the predicted.**

The portions of the observed concentrations that are contained within the envelope occur while a puff is not present. A concentration of zero is within the  $6\sigma$  envelope, and thus attempts to validate the model. This is not very helpful because it suggests that no release could have occurred and the model might satisfactorily predict that. In fact, this is proven as shown by the portion of time that occurs before the first puff arrives; it lies inside the envelope quite nicely.

### 3.3 Statistical Results

After running the stochastic model, certain conclusions can be reached by analyzing the statistical results. These include multiple suggestions that a stochastic model has potential to predict the path of a plume in low wind speed conditions, but not when coupled with a Lagrangian-based analysis program, such as SCIPuff.

The following statistics were computed: Fractional Bias (FB), Geometric Mean Bias (MB), Normalized Mean Square Error (NMSE), and the Geometric Variance (VG). A perfect model fit would have values of one for MG and VG and values of zero for FB and NMSE (Chang and Hanna 2004).

#### 3.3.1 Fractional Bias (FB)

Figure 3.3 shows the final FB computed using all the stochastic runs for the second ethylene release at 50 meters out from the release point. It is interesting to note that each puff is visible as a positive spike on the graph. Each time positive values are graphed, a puff is present; each time negative values are graphed, no puffs are present. The zero values show that the model predicts a lack of a plume quite well, so long as there actually is no plume present. After 11 seconds, the predicted plume begins to emerge, due to time-smearing values and contaminant release. We can conclude that this model is very sensitive to puff detection as shown in the steep jumps between negative and positive values. These jumps also suggest that the model should not be used to predict instantaneous data for a plume.

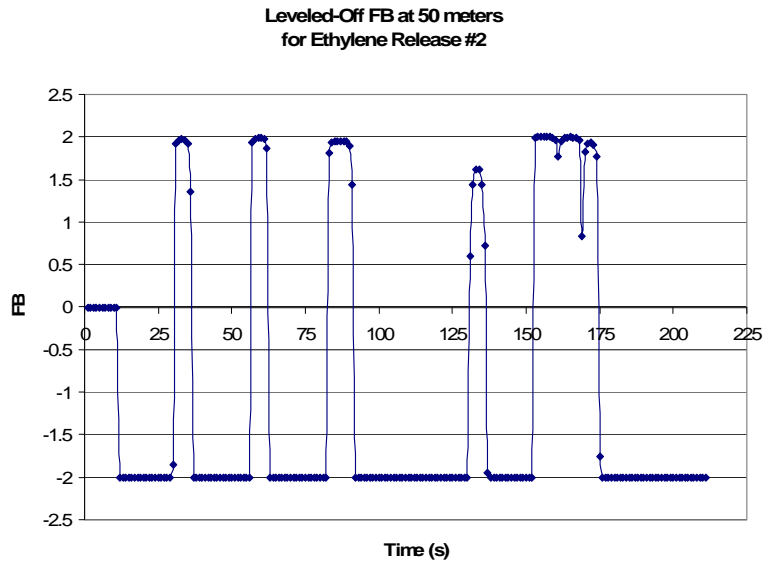


**Figure 3.3. Leveled-Off Fractional Bias (FB) Values of the Ethylene Release #2 at 50 meters. These values were taken at the point where additional statistical releases did not greatly change the value of the FB at each specific time-step. This was accomplished by generating each statistic iteratively throughout the generation phase of this evaluation.**

An ideal model fit would have an FB of zero (Chang and Hanna 2004). This model accomplishes this only before any plume hits or is predicted to hit. After the predicted plume “hits,” the FB values are either at a positive or negative value of two, depending on whether an observed puff is present (positive) or not (negative). The oscillating about zero actually has an average value of negative one (-1), thus proving that this stochastic model coupled with SCIPuff does not accurately predict plumes in low wind speed conditions.

### 3.3.2 Geometric Mean Bias (MB)

Each positive spike in Figure 3.4 represents a passing puff and each portion where the MB approaches zero, no contaminants “hit” the PIDs. The values for MB in an ideal model fit would be one, which is the case in Figure 3.4 only at times before 11 seconds.

This shows that the model does not accurately predict a plume similar to the observed plume and that it tends to zero when the predicted and observed plumes do not relate to each other at all; recall that values of zero were represented by values of  $10^{-20}$  due to the presence of natural logs in this statistic.

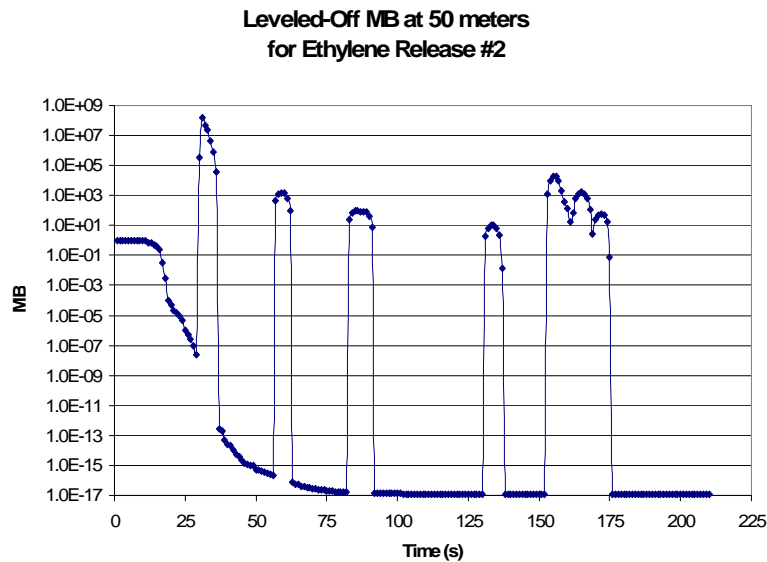


**Figure 3.4. Leveled-Off Geometric Mean Bias (MB) Values of the Ethylene Release #2 at 50 meters. These values were taken at the point where additional statistical releases did not greatly change the value of the MB at each time-step. This was accomplished by generating each statistic iteratively throughout the generation phase of this evaluation. The y-axis is log-scale.**

### 3.3.3 Normalized Mean Square Error (NMSE)

An ideal model fit would show the NMSE value as zero. This was not accomplished by the model except for the un-plotted portion during the first 11 seconds, before any puffs reached the PIDs. These zero values are not plottable because the y-axis is log scale. The rest of the release time is punctuated by short puffs of the contaminant plume passing by, as shown by the downward spikes in Figure 3.5. It is evident that this statistic could be accurate if the PIDs continually registered contaminant “hits” with

values above zero. This is shown by the fact that when a plume is passing, the NMSE values are much closer to the ideal zero than when they are not. Due to the majority of the release time being without plume detection, the average value for the NMSE at 50 meters is  $5.7 \times 10^{16}$ . NMSE tends to  $1 \times 10^{17}$  when the predicted and observed plumes are not similar, further suggesting SCIPuff does not model this low wind speed situation well.

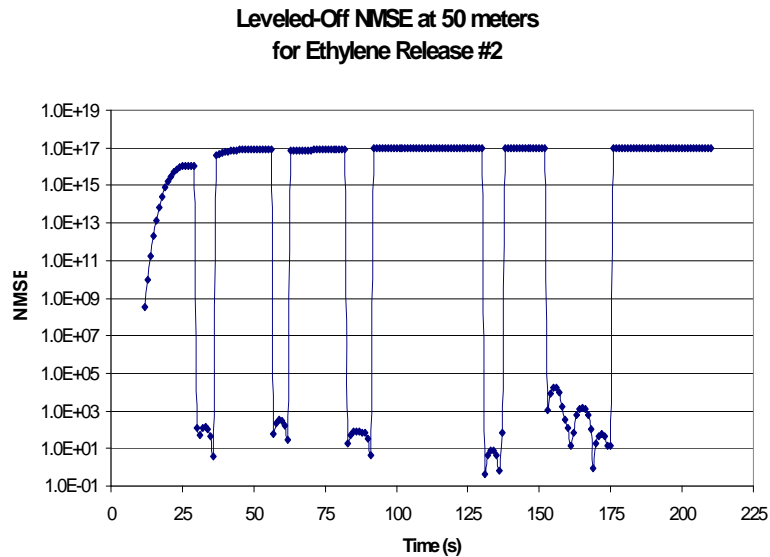


**Figure 3.5. Leveled-Off Normalized Mean Square Error (NMSE) Values of the Ethylene Release #2 at 50 meters. These values were taken at the point where additional statistical releases did not greatly change the value of the NMSE at each time-step. This was accomplished by generating each statistic iteratively throughout the generation phase of this evaluation. The y-axis is log-scale.**

It is also interesting to note the somewhat gradual climb of NMSE values between 12 and 26 seconds. This is due to the fact that the predicted concentrations began to appear at the former time and the observed concentrations did not show up until the latter time mentioned. Thus, we can see the great impact the predicted concentration has on the

statistics. It is, therefore, imperative that an accurate model be developed to predict the observed plume.

### 3.3.4 Geometric Variance (VG)

The VG describes how much spread there is in the data for an experiment. As shown in Figure 3.6, these data have quite a bit of spread. Figure 3.6 is shown with the y-axis values in log-scale so that each of the five puffs can be seen. The gaps between the data points are where the VG values were equal to zero, and therefore, are un-plottable on this particular graph. These should not concern us though, for the ideal model fit would have values of one for VG. This clearly only occurs until the 11 second mark, where the predicted plume begins to be “detected.”

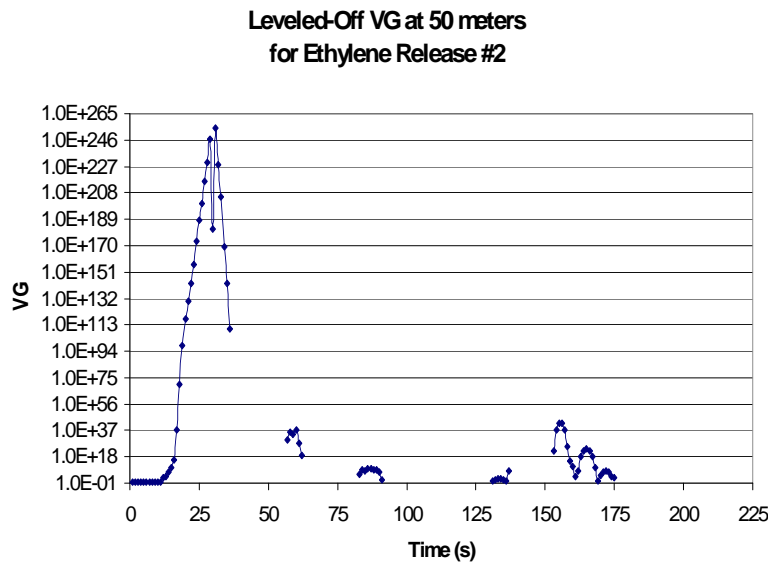


**Figure 3.6. Leveled-Off Geometric Variance (VG) Values of the Ethylene Release #2 at 50 meters. These values were taken at the point where additional statistical releases did not greatly change the value of the VG at each time-step. This was accomplished by generating each statistic iteratively throughout the generation phase of this evaluation. The y-axis is log-scale.**

### 3.3.5 General Statistics Remarks

I believe the main reason for the non-ideal statistics is the lack of vertical motion and turbulence in the SCIPuff model. At the downwind distances where the PIDs were placed, the horizontal eddies should have had enough time to be fully mixed, if we assume the horizontal eddies and dispersion are traveling at 10-20% of the advective currents. At the same time, the vertical motion component could be on the same order of magnitude as advection. This would cause more upward motion than is predicted by standard air models, including SCIPuff, which is currently none.

A solution for this would be to create a model that could take all three dimensions into account in order to accurately model the plume. This might require starting from the Navier-Stokes equations and working forward to be able to assess a volume of air and everything that moves inside it.

Another reason why the statistics do not match up is that SCIPuff is designed to work with values that are the average for a portion of time. I implemented SCIPuff to work with instantaneous data and predictions, which was not successful.



## 4 Conclusions

It was found that stochastically modeling chemical plume releases in low wind speed conditions is not accurate. This was expected because below 2 m/s, plumes no longer have a Gaussian distribution and are difficult to predict.

Each of the examined statistics pointed to the case that this stochastic model, when coupled with SCIPuff, does not accurately predict the concentration of contaminant plumes in low wind speed conditions. None of the statistics were at the values associated with ideal model fits; and none were particularly close either. In fact, the model only accurately predicts that there will be no plume when no plume is present, so long as no plume is ever present.

It is possible, and even probable, that stochastic modeling of contaminant plumes will work, when coupled with a model that is accurate for low wind speed conditions, including wind data for all three dimensions and other important characteristics of wind.

An unexpected finding is the fact that 2-D wind data alone is not enough to accurately model wind movement in low wind speed conditions. Including the third spatial dimension of wind data would probably yield better results. This is significantly different from conditions with wind speeds above 2 m/s, where the horizontal and lateral movements are much greater than the vertical movements. When planning future

experiments, attention should be paid to obtaining a good representation of the 3-D wind profile and attempting to model it.

In order to correctly model plumes at these low wind speeds, more research is needed. A good starting point would be to build off of Pasquill's work, done in the 1960s, using current computing power and understanding of aerodynamics, particle movement, and dispersion.

An accurate model would aide in many portions of life, including military concerns, chemical leaks and/or releases, city planning, and emergency response. Therefore, it is recommended that more funding be put into this field of study in order to obtain long-awaited results and that the existing models make their limitations known to their users.

## REFERENCES

- Anfossi, D., Brusasca, G., and Tinarelli, G. (1990). "Simulation of Atmospheric Diffusion in Low Windspeed Meandering Conditions by a Monte Carlo Dispersion Model." *Il Nuovo Cimento* 13C: 995-1106.
- Arya, S. P. (1999). Air Pollution Meteorology and Dispersion. New York, NY, Oxford University Press.
- Barad, M. L. ed. (1958). Project Prairie Grass, A Field Program in Diffusion. Geophysical Research Papers. Bedford, Massachusetts, Atmospheric Analysis Laboratory, Geophysics Research Directorate, Air Force Cambridge Research Center, Air Research and Development Command, United States Air Force: 280.
- Briggs, G. A. (1973). Diffusion Estimation for Small Emissions. Oak Ridge, TN, Air Resources Atmospheric Turbulence and Diffusion Laboratory, U. S. National Oceanic and Atmospheric Administration: 59.
- Briggs, G. A. (1975). Plume Rise Predictions. Lectures on Air Pollution and Environmental Impact Analysis. D. A. Haugen, ed. Boston, MA, American Meteorological Society: 59-111.
- Brusasca, G., Tinarelli, G., and Anfossi, D. (1992). "Particle Model Simulation of Diffusion in Low Wind Speed Stable Conditions." *Atmospheric Environment* 26A: 707-723.
- Chang, J. C. and Hanna, S. R. (2004). "Air quality model performance evaluation." *Meteorology and Atmospheric Physics* 87: 167-196.
- Cirillo, M. C. and Poli, A. A. (1992). "An Intercomparison of Semi-empirical Diffusion Models under Low Wind Speed, Stable Conditions." *Atmospheric Environment* 26A(5): 765-774.
- Cox, W. M. a. Tikvart, J. A. (1990). "A Statistical Procedure for Determining the Best Performing Air Quality Simulation Model." *Atmospheric Environment* 24A(9): 2387-2395.
- Cramer, H. E., Record, F. A., and Vaughan, H. C. (1958). "The study of the diffusion of gases or aerosols in the lower atmosphere." Cambridge, MA, Massachusetts Institute of Technology.
- Dobbins, R. A. (1979). Atmospheric Motion and Air Pollution. New York, John Wiley and Sons.
- Ermak, D. L., Chapman, R., Goldwine, C., Goveia, J., and Rodean, H. C. (1989). Heavy Gas Dispersion Test Summary Report. Tyndall AFB, FL, Lawrence Livermore

- National Laboratory, Air Force Engineering & Services Center (AFESC), Engineering & Services Laboratory at Tyndall AFB, FL.
- Etling, D. (1990). "On Plume Meandering Under Stable Stratification." *Atmospheric Environment* 24A: 1979-1985.
- Fuquay, J., Simpson, C. L., and Hinds, W. T. (1964). "Prediction of environmental exposures from sources near the ground based on Hanford experimental data." *Journal of Applied Meteorology* 3: 761-770.
- Gifford, F. A. (1959). Statistical Properties of a Fluctuating Plume Dispersal Model. Symposium on Atmospheric Diffusion and Air Pollution, Oxford University, Academic Press.
- Gifford, F. A. (1960). "Peak to average concentration ratios according to a fluctuating plume dispersion model." *International Journal of Air Pollution* 3: 253-260.
- Gifford, F. D. (1975). Atmospheric Dispersion Models for Environmental Pollution Applications. Lectures on Air Pollution and Environmental Impact Analysis. D. A. Haugen. Boston, MA, American Meteorological Society: 35-58.
- Hanna, S. R. (1983). "Lateral Turbulence Intensity and Plume Meandering During Stable Conditions." *Journal of Climate and Applied Meteorology* 22: 1424-1231.
- Hanna, S. R. (1986). "Spectra of Concentration Fluctuations: the Two Time Scales of Meandering Plume." *Atmospheric Environment* 20: 1131-1137.
- Hanna, S. R. (1989). "Confidence Limits for Air Quality Model Evaluations, as Estimated by Bootstrap and Jackknife Resampling Methods." *Atmospheric Environment* 23(6).
- Hanna, S. R., Strimaitis, D. G., and Chang, J. C. (1991). Volume I. User's Guide for Evaluating Hazardous Gas Dispersion Models. Hazard Response Modeling Uncertainty (a Quantitative Method), Air Force Engineering and Service Center.
- Hanna, S. R., Strimaitis, D. G., and Chang, J. C. (1991). Volume II. Evaluation of Commonly-Used Hazardous Gas Dispersion Models. Hazard Response Modeling Uncertainty (a Quantitative Method), Air Force Engineering and Service Center.
- Haugen, D. A. (1959). Project Prairie Grass, a field program in diffusion. Geophysical Research Papers, U.S. Air Force Cambridge Research Center. No. 59, Vol. III.
- Jones, N. (1998). "Environmental Modeling Research Laboratory (EMRL)." 2007, from <http://www.emrl.byu.edu/home.htm>.
- Kristensen, L., Jensen, N. O., and Peterson, E. L. (1981). "Lateral Dispersion of Pollutants in a Very Stable Atmosphere - The Effect of Meandering." *Atmospheric Environment* 15: 837-844.
- LaGrega, M., Buckingham, P. L., and Evans, J. C. (2001). Hazardous Waste Management. Boston, MA, McGraw Hill.
- Moore, G. E., Milich, L. B., and Liu, M. K. (1988). "Plume Behaviour Observed using Lidar and SF6 Tracer at a Flat and Hilly Site." *Atmospheric Environment* 22(8): 1673-1688.

- Nepf, H. (2006). Class Notes. MIT's 1.060 Class. Cambridge, MA.
- Nickola, P. W. (1977). The Hanford 67-Series: A Volume of Atmospheric Field Diffusion Measurements. Battelle, Washington, Pacific Northwest Laboratories.
- Oettl, D., Almbauer, R. A., and Sturm, P. J. (2001). "A New Method to Estimate Diffusion in Stable, Low-Wind Conditions." *Journal of Applied Meteorology* 40(2).
- Sagendorf, J. F. and Dickson, C.R. (1974). Diffusion under Low Wind-speed, Inversion Conditions. Technical Memorandum ERL ARL-52, U.S. Nat. Oceanic and Atmos. Admin.
- Sawyer, P. S. (2007). Atmospheric Dispersion Model Validation for Low Wind Speed Conditions. Department of Environmental Studies. Las Vegas, NV, University of Nevada. Master of Science: 64.
- Sharan, M. and Yadav, A. K. (1998). "Simulation of Experiments Under Light Wind, Stable Conditions by a Variable K-Theory Model." *Atmospheric Environment* 32(20): 12.
- Sharan, M., Yadav, A. K., Singh, M. P., Argarwal, P., and Nigam, S. (1996). "A Mathematical Model for the Dispersion of Air Pollutants in Low Wind Conditions." *Atmospheric Environment* 30(8): 1209-1220.
- Sharan, M., Yadav, A. K., and Modani, M. (2002). "Simulation of short-range diffusion experiment in low-wind convective conditions." *Atmospheric Environment* 36(11): 6.
- Sharan, M. and Modani, M. (2005). "An Analytical Study for the Dispersion of Pollutants in a Finite Layer under Low Wind Conditions." *Pure & Applied Geophysics* 162(10): 32.
- Sharan, M., McNider, R. R., Gopalaikrishnan, S. G., and Singh, M. P. (1995). "Bhopal Gas Leak: A Numerical Simulation of Episodic Dispersion." *Atmospheric Environment* 29: 2061-2074.
- Sharan, M., Modani, M., and Yadav, A. K. (2003). "Atmospheric Dispersion: An Overview of Mathematical Modeling Framework." *Proc. Indian Nat. Sci. Academy* 69A: 725-744.
- Sharan, M. and Gopalakrishnan S. G. (2003). "Mathematical Modeling of Diffusion and Transport of Pollutants in the Atmospheric Boundary Layer." *Pure & Applied Geophysics* 160: 38.
- Sharan, M. and Gupta, S. (2002). "Two-dimensional Analytical Model for Estimating Crosswind-integrated Concentration in a Capping Inversion: Eddy Diffusivity as a Function of Downwind Distance from the Source." *Atmospheric Environment* 36: 9.
- Sharan, M., Singh, M. P., and Yadav, A. K. (1996). "A Mathematical Model for the Atmospheric Dispersion in Low Winds with Eddy Diffusivities as Linear Functions of Downwind Distance." *Atmospheric Environment* 30(7): 9.

- Slade, D. H. (1968). *Meteorology and Atomic Energy*. Division of Technical Information, U. S. Atomic Energy Commission, Oak Ridge, TN.
- Sugiyama, G., Nasstrom, J. S., and Baskett, R. L. (November 14, 2003). *Operational Systems for Emergency Preparedness and Response*. Symposium on Planning, Nowcasting, and Forecasting in the Urban Zone
- 84th American Meteorological Society Annual Meeting. Seattle, WA, Lawrence Livermore National Laboratory, University of California.
- Sykes, R. I., Parker, S.F., Henn, D.S., Cerasoli, C.P., and Santos, L.P. (Sept. 1998). *PC-SCIPIUFF Version 1.2PD Technical Documentation*, Titan Corporation. Titan Research & Technology Division. ARAP Group.
- Tangirala, R. S., Rao, K. S., and Hosker, R. P. (1992). "A Puff Model Simulation of Tracer Concentrations in the Nocturnal Drainage Flow in a Deep Valley." *Atmospheric Environment* 26A(2): 11.
- Van der Hoven, I. (1976). "A Survey of Field Measurements of Atmospheric Diffusion under Low-wind-speed Inversion Conditions." *Nuclear Safety* 17(2): 8.
- Yadav, A. K. and Sharan, M. (1996). "Statistical Evaluation of Sigma Schemes for Estimating Dispersion in Low Wind Conditions." *Atmospheric Environment* 30(14): 12.

## **Appendix A. Details of Extending Sawyer's Experiment**

I obtained the data used in this research from Sawyer and National Security Technologies, LLC (NSTec). The experiment from which this data is taken is explained in detail in Sawyer (2007). I performed two types of analyses on the data I obtained. The first was a graphical representation of each chemical release plume developed using a software program called GMS. The second analysis was a stochastic analysis which involved original codes and a plume modeling program called SCIPuff.

All programs used for data manipulation in this project were written in a bash shell script with calls to sed, awk, and Octave. Octave is a free UNIX program similar to MATLAB that can run on Windows machines. These languages and programs were chosen because of their ability to manipulate data as ASCII files, accurately and efficiently without the complications of GUIs. Writing the programs took some time, but this process was more efficient than additional by-hand manipulation in Excel.

### **4.1 GMS Analysis**

To prepare the data for animation in GMS, a large quantity of manipulation in Excel and UNIX programming languages were required.

The first step was to extract the PID data (time and concentration) from Sawyer's data files. Data from each release sequence occupied its own spreadsheet, from which

the pertinent data were extracted and placed in a new spreadsheet. These files were labeled '<Chemical>Seq<Sequence Number>' and were called in the '<Chemical>LongPull2' program, which created separate files for each PID with its associated times and concentrations. A program called 'Main' was then run, which created a file for each chemical sequence that included the expanded time vector (in decimal hours) and the interpolated concentration for each PID. The interpolation scheme called 'pchip' was chosen to eliminate the stair-step effect 'nearest' gave. Due to the need for some type of interpolation to satisfactorily match the concentration data with the expanded time data, the scheme that produced the smoothest data was chosen; this matched my understanding of plume behavior for this application. To prepare the data for a spatial interpolation in GMS, manual manipulation was required.

The extracted data were transposed from increasing time down rows and PID numbers across columns to increasing time across columns and PID numbers down rows. Each PID also needed a location for GMS to graph it properly. This was done by overlaying the PID layout on a 2000x2000 cell grid that was centered on the release point (ground zero). Each grid cell was equivalent to 0.1 meter square on the actual PID layout. Each PID had a unique x- and y-value for its location.

Once this was done, the time separations needed to be standardized. Originally, there was a five to eight second separation between PID sampling with few of the times matching between different PIDs. This problem was solved by resizing the time-scale to one second increments (which GMS required) and placing the PID sample concentration data at the time it was taken. Each row with time data was then deleted, leaving only the concentrations (in ppm) for each PID and the corresponding time column. This value

was assumed constant for the next period of time until a new sample was taken and the value changed. The concentration values before the first sample taken were assumed to be zero. See Figure A.1 for an illustration of the process of filling-in these spreadsheets.

PID	X (0.1 m)	Y (0.1 m)	conc	18:40:00	18:40:01	18:40:02	18:40:03	18:40:04	18:40:05	18:40:06	18:40:07	18:40:08	18:40:09	18:40:10	18:40:11	18:40:12
				13/02/2007 18:40:00	/02/2007 /02/2007	/02/2007 /02/2007	/02/2007 /02/2007	/02/2007 /02/2007	/02/2007 /02/2007	/02/2007 /02/2007	/02/2007 /02/2007	/02/2007 /02/2007	/02/2007 /02/2007	/02/2007 /02/2007	/02/2007 /02/2007	/02/2007 /02/2007
1	1000	1100				0							0			
3	1100	1000				0							0			
53	1000	900				0							0			
4	900	1000				0							0			
5	1000	1250				0							0			
6	1176.777	1176.777					0								0	
7	1250	1000					0								0	
8	1176.777	823.2233					0								0	
9	1000	750	0	0	0	0	0	0	0	0	0	0	0	0	0	0
13	823.2233	823.2233	0	0	0	0	0	0	0	0	0	0	0	0	0	0
14	750	1000	0	0	0	0	0.1455	0.1455	0.1455	0.1455	0.1455	0.1455	0.1455	0	0	0
17	823.2233	1176.777						0						0		
18	1000	1500						0							0	
19	1353.553	1353.553						0							0	
20	1500	1000						0							0	
21	1353.553	646.4466						0							0	
23	1000	500						0							0	
25	646.4466	646.4466							0						0	
27	500	1000							0							0
28	646.4466	1353.553							0							0
32	1000	2000							0							0
33	1382.683	1923.88							0							0
34	1707.107	1707.107	0								0					
35	1923.88	1382.683	0								0					
36	2000	1000	0								0					
37	1923.88	617.3166									0					

**Figure A.1. Example of Excel Data Manipulation for GMS. Each PID was listed by number and location and their concentrations corresponded to times on the upper row. Each observed concentration (in ppm) was placed on its original time and assumed constant until the next measurement was taken; then the pattern repeated.**

A zero-concentration data point was added to the time-step after the end of each of the PID sequence measurements if they ended in a non-zero and then a zero data point. If the PID measurements ended in a non-zero value, a zero value was added to the next logical time-step and another zero beyond that. These helped smooth out the interpolated data curve. Before correcting for this, the data extrapolation would yield unrealistic values.

Once the spreadsheets were complete, the data could be opened in GMS as an imported file and saved as a \*.gpr file. In GMS, the PIDs' concentration data were

interpolated to a 2-D surrounding grid with time becoming the third dimension. An image of the grid and PID layout is shown in Figure A.2.

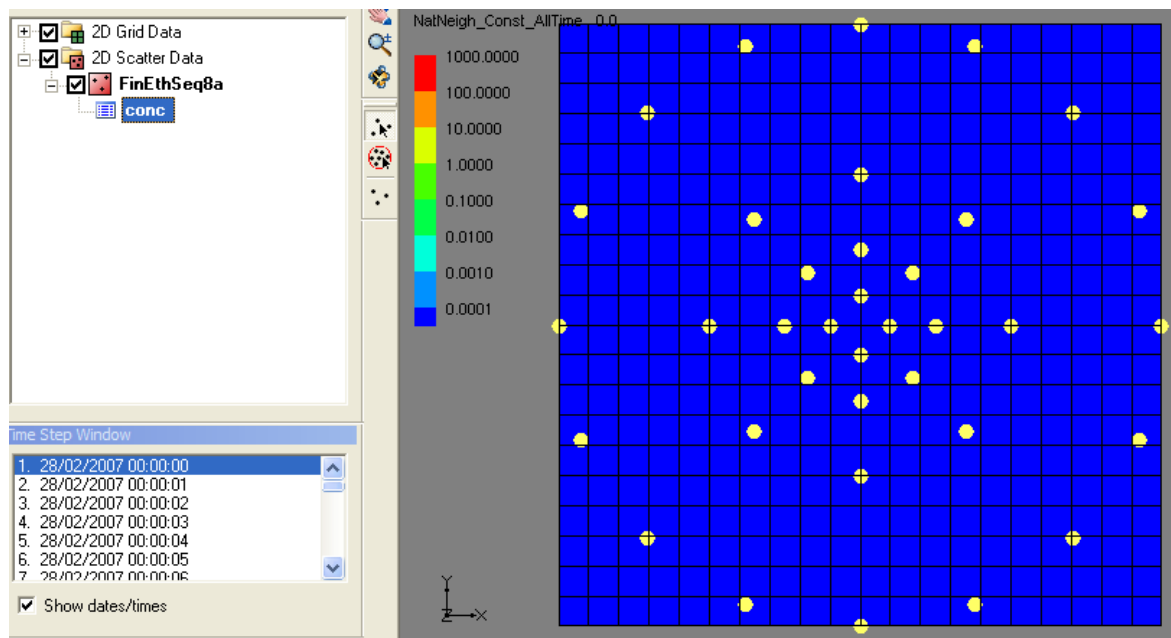


**Figure A.2. GMS Interpolated 2-D Grid of PIDs with Time-Step Window.**

The interpolation scheme that mapped the measured PID concentrations to the 2-D grid points created the data used to form the concentration plume contours, so it was important to choose an appropriate scheme. There were various interpolation schemes that could be used for interpolating data in the areas between the PIDs. The Natural Neighbor interpolation scheme using the Gradient nodal function computed from all scatter points with extrapolation beyond the convex hull was tried and produced patterns that appeared mostly symmetrical and that had “no hit” holes. Around the PIDs were colors showing hits in the area, but the PIDs were registering zero. This meant that pockets of zero appeared within clouds of measurable concentration and that is not an accurate visualization of the plume since it does not follow the physical constraints of air

transport. The Natural Neighbor interpolation scheme using the Gradient nodal function computed at the Natural Neighbor scatter points with extrapolation beyond the convex hull produced peanut-shaped plumes in areas that were supposed to have a concentration of zero. This, as the previously tried interpolation, was not an accurate visual model of the plume. This peanut effect was nullified by using the Natural Neighbors interpolation scheme using a Constant nodal function with extrapolation beyond the convex hull. This is the scheme that was used in the analysis. Thus, with the PIDs correctly mapped to the 2-D grid, the related contours would also be accurate. These contours formed an animation which showed the progression of the data throughout time. An example of a 2-D grid with contours for one time-step is shown in Figure A.3.

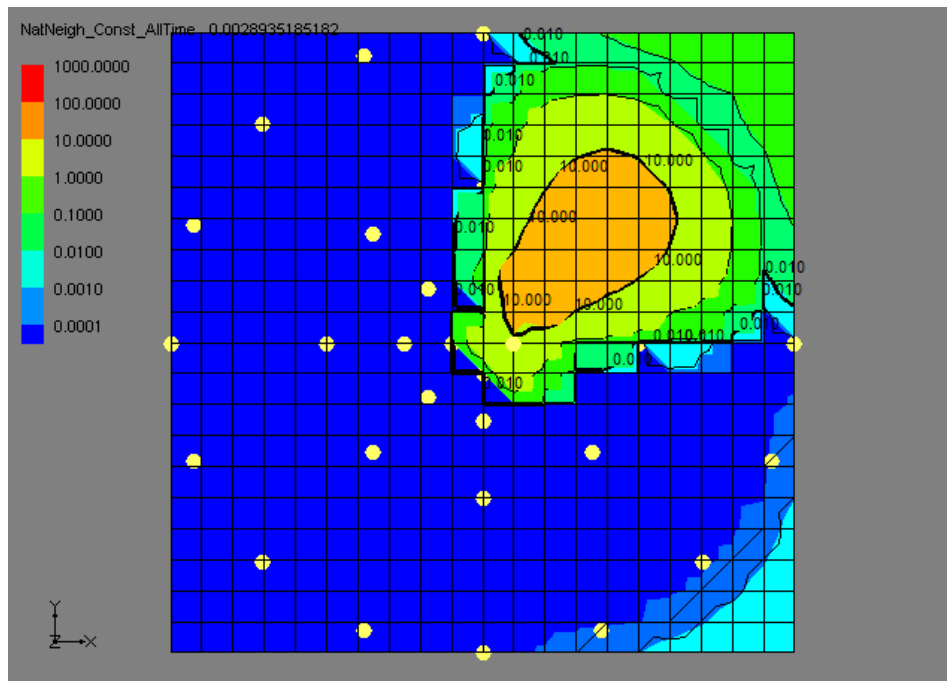


**Figure A.3. (Repeat of Figure 2.4.) GMS Interpolated 2-D Grid of PIDs with Contaminant Plume Contours. On the left is the logarithmic scale for the PID sample concentrations.**

## 4.2 SCIPuff Analysis

Because SCIPuff was configured to only calculate outcomes when based on a plume traveling in one direction, the centerline of the plume needed to be found. The centerline was assumed to be the maximum concentration detected at each PID ring at each time-step, such that for each time-step there is a concentration at 10, 25, 50, and 100 meters; each of which are the maximum measured for that distance at that time-step. There was only one instance where the maximum concentration was observed at two different locations on the same distance ring. This anomaly, as well as the normal readings, was nullified by the fact that the centerline plume was then assumed to be straight, intersecting each of the distances with the maximum measured concentration at that time-step. This may not be accurate, but with the sparsely populated PID field, this was as close to the centerline of the plume that could reasonably be obtained. Thus, the SCIPuff analysis looks more at concentration fluctuations over the distances over time than the actual plume path over a 2-D spatial plane over time. More work or research will need to be done (with a denser array of sensors) to get an accurate record of how the Centerline plume travels over space and time. This model was aimed at producing conservative estimates of concentrations for safety evaluations.

The programs written for this portion of the analysis take the observed fluctuations of each chemical release sequence and compare their SCIPuff results to that found by the experimental centerline, as described above. There were three main programs that accomplished the task: 'Statistics.m', 'GenStatVars', and 'SMPRun'. 'Statistics.m' calculated all the statistics from the results of running SCIPuff. 'GenStatVars' generated the statistical values for the initial SCIPuff variables and

‘SMPRun’ acted as the main program, calling the other two and processing all gathered information in a loop structure. The first two programs were written in Octave and the last was written in a bash shell that called sed, awk, and Octave.

Each program brought about its own challenges. ‘Statistics.m’ was called from inside the ‘SMPRun’ loop, but could not pass parameters easily back to the shell script. Values were therefore passed using files. ‘GenStatVars’ required extensive background research to understand each of the stochastic variables and what their logical value ranges would be. ‘SMPRun’ required learning four new programming languages and attempting to make them all work together to accomplish the task.

In order to pass parameters in Octave, the current run index, ‘i’, was saved in a separate file inside the main loop of ‘SMPRun.’ ‘i’ was the loop index for this main loop and was automatically updated by the loop structure. The file was created by using the ‘dlmwrite’ function as the first command inside the loop. At the start of the octave program, the file was opened by copying its contents into a temporary variable using the ‘dlmread’ function. This allowed new columns in the ‘Statistics.m’ matrices to be added; one with each looping in the ‘SMPRun’ program.

Writing the ‘Statistics.m’ file was challenging due to the fact that zero is a valid measurement in the experiment, but is not valid in some of the statistics, such as the inner mathematical steps involving natural logs and the Normalized Mean Square Error (NMSE). These logic errors were observed when each of the inner steps and complete statistical equations were implemented in a straight list, without any conditional statements.

The natural logs posed a problem because the natural log of zero is equal to negative infinity ( $\ln(0) = -\infty$ ). This, in and of itself would not have been a problem, but the statistics were being developed iteratively. This meant that during each run through the loop, the  $i^{\text{th}}$  vector (which is the current run vector) was solved for and its value was equal to the current value plus the value in the (i-1) vector (the last intermediate statistics column). Thus, negative infinity ( $-\infty$ ) plus a small (or large number, for that matter) was still equal to negative infinity ( $-\infty$ ). Regardless of the value of the observed or predicted concentration, the statistics that had a natural log function in them were always equal to negative infinity ( $-\infty$ ).

This natural log issue was solved by declaring all zero values to be equal to  $10^{-20}$ . This allows the computer to calculate any computation, essentially calculating in a value of zero. This is acceptable due to the fact that a measured value of zero is actually equal to some value between zero and the minimum measuring limit of the equipment. This solution to the “zero problem” also solved the challenge associated with NMSE.

The NMSE provided a “division by zero” challenge. When the average measured concentration was greater than zero, NMSE could be solved for without a problem. However, when the average measured concentration was equal to zero, the denominator of NMSE was also equal to zero and NMSE was equal to infinity ( $\infty$ ). This value of infinity ( $\infty$ ) was not wrong, per say, but the warning message was appeased by the previously mentioned solution of changing all values of zero to the value of  $10^{-20}$ .

Both the natural log and NMSE issues were non-issues when the measured concentration of the run was greater than zero, but by forcing all values to be greater than zero, an error message was avoided and their vectors were simplified.

There is also a check for equal vector lengths in ‘Statistics.m’, which ensures that there is the same amount of observed data as there is predicted data. If the vectors are not the same length, an error message is displayed, but the program continues. It is important to check for this error message and to not run the ‘Statistics.m’ program all the way to the end of the shorter vector. This will give an even worse error about the math not being able to happen and will just be a waste of time because it means the two columns are not for the same run.

Each statistic calculated in ‘Statistics.m’ was simplified into smaller portions such that the calculations could be checked step-by-step, as previously mentioned. This allowed for errors to be located quickly and effortlessly when the vectors calculated in Octave were compared to the hand-calculated vectors in Excel.

One of the last steps in ensuring the statistics were readable was to transpose their matrix. When the statistic vectors were combined into a statistic matrix, they were calculated and written as rows. This did not prove to be a problem when the matrix transpose (matrix’) was written to the file that was then saved into the appropriate folder.

‘Statistics.m’ was run for each of the four sets of predicted values associated with the distances in the PID array. The column extracted from the measured concentration file was incremented for each distance, 10, 25, 50, and 100 meters. Once the statistics were calculated for a particular distance for the particular run, they were added to a file specific to that distance. Each run of ‘Statistics.m’ updated the matrix in that file with the incremental statistics so the changes could be seen. This allowed me to see when the statistics leveled out, and an analysis could be performed.

Within ‘GenStatVars’, two of the variables changed are  $\sigma_z$  and  $\sigma_y$ . They are the vertical and horizontal dispersion coefficients,  $\sigma_z$  and  $\sigma_y$ , respectively, and were determined by looking at the Pasquill-Gifford-Turner (PGT) charts for dispersion coefficients as a function of atmospheric stability category and downwind distance. These charts are part of the PGT classification scheme because they worked on categorizing the stability of the atmosphere and found that the dispersion coefficients were dependant upon atmospheric stability and downwind distance. Thus, finding the anticipated values of  $\sigma_z$  and  $\sigma_y$  is quite simply a matter of using the PGT charts and the known downwind distance and the atmospheric stability class (A-F). Our distance (x) values ranged from 10 to 100 meters to make sure these values were valid for each of the PID rings for the experiment. Remember that though the plume was calculated with four PIDs, each was located on one of the PID rings so those distance values never change.

The other variables generated in ‘GenStatVars’ were the wind speed, the amount of mass released in the plume simulation (CMASS), the release height, and the time-step (delta). The wind speed was determined by taking a value from the Gaussian curve created by centering the function over the average observed wind speed and using the calculated standard deviation for the run. This is shown below.

```
#Wind Speed
#Use avg wind speed for that sequence as found in measured results
#Gaussian, centered over the average of the sequence
stdev= #value of the Std. dev unique to that seq. from measured data
SeqWS= #avg wind speed of sequence being run
WindSpeed=normal_rnd(SeqWS,stdev) #randomly generated value between 0 and 1
```

The CMASS was generated by taking a percentage of the actual released mass with a uniform distribution between  $\pm 10\%$  of the actual mass released. This percentage was

determined by the use of a random number. The code used for this variable generation is shown below.

```
#CMASS
#+ or - 10% of what Pat Sawyer had; changes for each sequence
#Random number to give an even distribution for + or - 10% of each seq.
#see CMASS.xls for values for each sequence (use kg of CMASS)
PatValue=0.083333 #manual updates per sequence
CMASS=(rand)*(0.2*PatValue)+(0.9*PatValue);
```

The release height and the time-step were both set to constant values of two meters and one second, respectively. This was the actual release height and a convenient time-step that allowed the desired level of detail to be examined.

3 spaces before  
and after  
figures/tables and  
their caption